

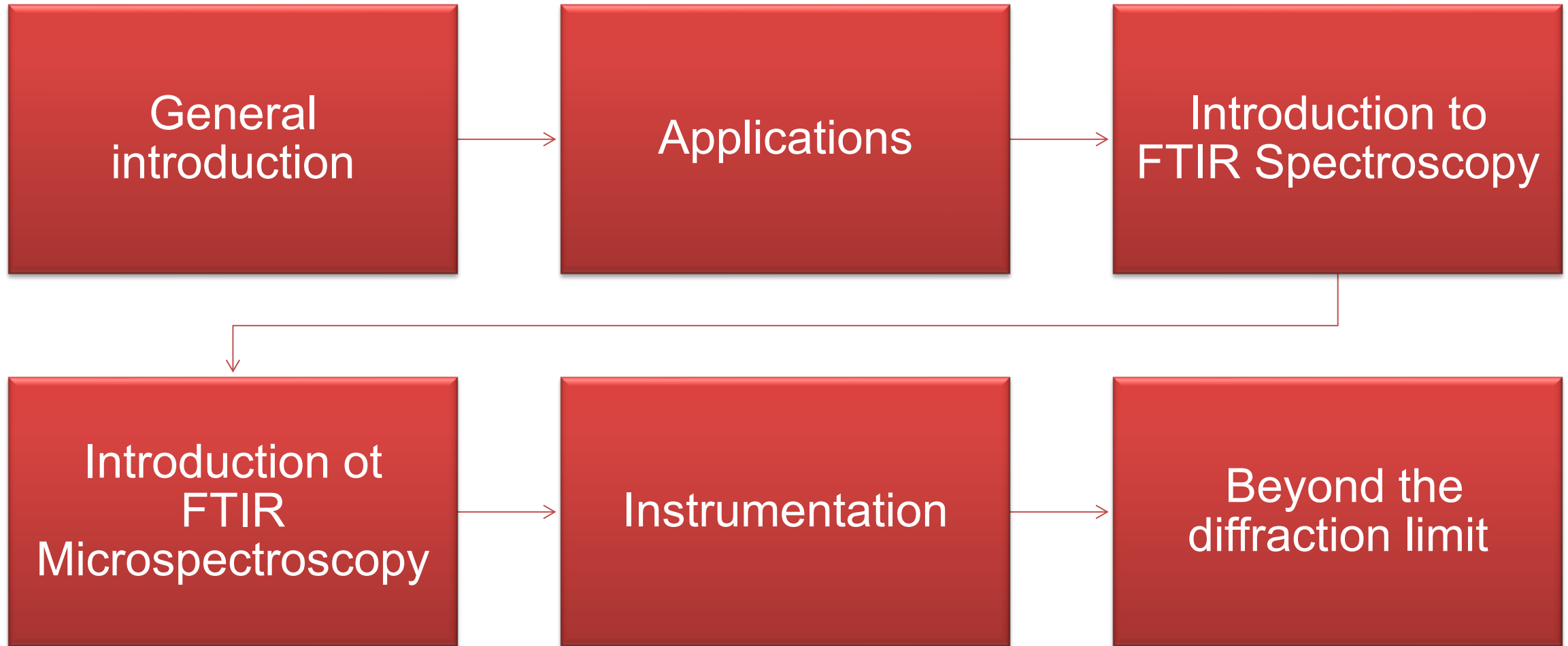
SYNCHROTRON INFRARED MICROSPECTROSCOPY

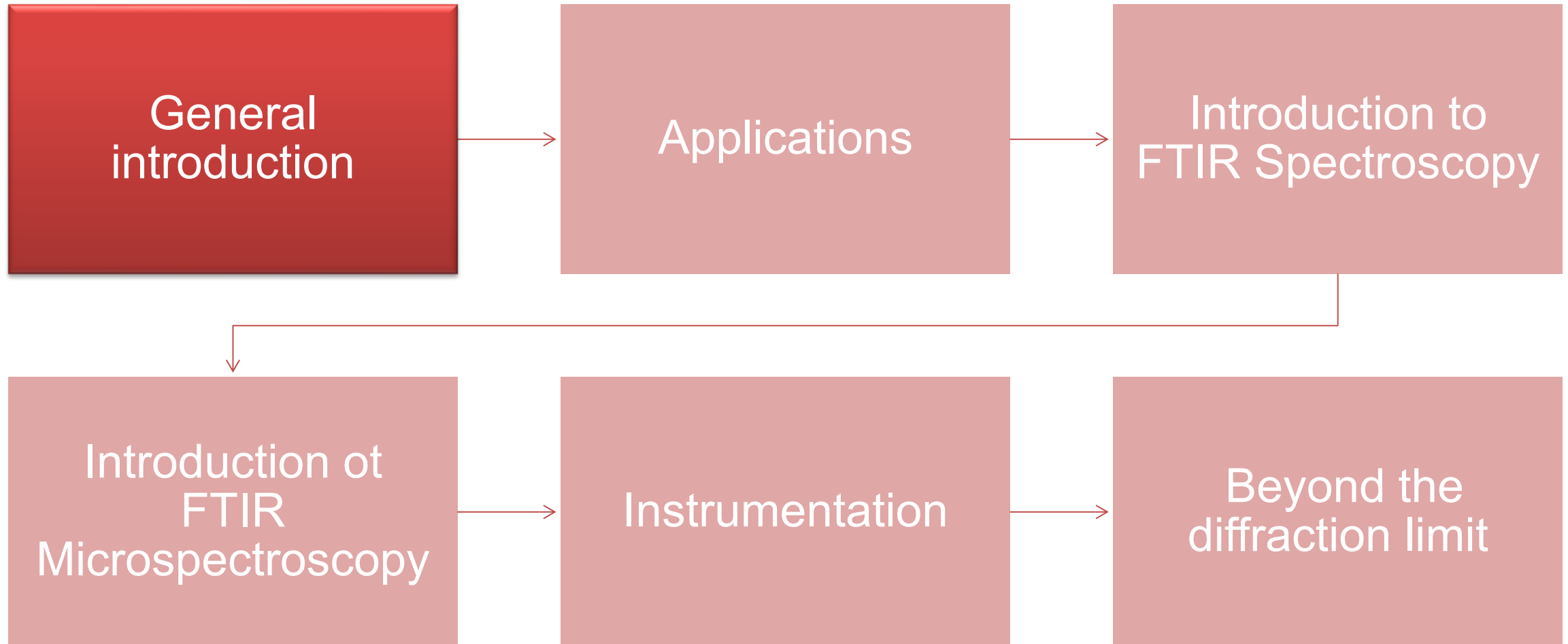
Christophe Sandt
SMIS beamline
Synchrotron SOLEIL



School on Synchrotron Light Sources and Their Applications
Smr 4205
January 13, 2026







WHY USE SYNCHROTRON FOR INFRARED MICROSPECTROSCOPY?

1) HIGH SPATIAL RESOLUTION

- Conventional μ FTIR (thermal source): 20-25 μm best resolution (**high flux**, **low brilliance**)
- Synchrotron Radiation μ FTIR: 3-20 μm resolution (**low flux**, **high brilliance**)

2) ULTRABROADBAND SOURCE

- The synchrotron source covers the whole IR domain:
 - Far-IR 25-900 μm
 - Mid-IR: 2.5-25 μm
 - Near-IR: 1-2.5 μm
- Thermal sources only cover part of the far-IR and near-IR
- IR lasers are narrow-band

3) BECAUSE IR SPECTROSCOPY **CAN** or **MAY** ANSWER YOUR SCIENTIFIC QUESTION

- 1) Chemical composition of the sample
- 2) Chemical phase of the sample
- 3) Spatial distribution of the molecules in the sample
- 4) Molecular conformation or orientation in the sample
- 5) Interaction of the sample and its environment
- 6) Measuring the sample under **constraint** (temp., press., stretch., irradiation, aging, reacting ...) in **real-time**
- 7) Sample must be measured **without contact** or **non-destructively**

- 1) Sample must be **chemically heterogeneous**.
 - No gas or liquid (unless there is a liquid phase separation)
 - Heterogeneity at the **micron scale** for **microspectroscopy**
 - Heterogeneity at the **nano-scale** for **nano-IR** techniques

- 2) **Small samples** that can not be measured at lower resolutions
 - Microparticles
 - Animal or plant cells
 - Microfibers...

- 3) Sample must be in a suitable form:
 - **Thin** for transmission measurements (few μm to few tens of μm)
 - Can be naturally thin
 - Can be thin-sectioned
 - Can be compressed in a **Diamond Compression Cell** -► may induce loss of spatial organization

 - **Flat** and **reflective** for reflection measurements

 - **Flat, smooth** and **solid** for Attenuated Total Reflection (ATR) measurements

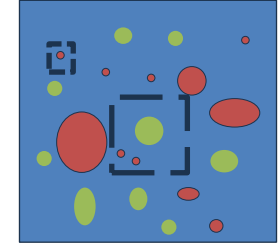
- 4) Sample **preparation** is paramount and must be **specifically adapted** to the technique
 - 1) Thin sections
 - 2) Polishing
 - 3) Embedding/no embedding
 - 4) Chemical fixation
 - 5) Flattening
 - 6) ...

- 5) **Experimental plan**
 - IR spectroscopy is most often an indirect technique:
 - Need appropriate controls for comparison
 - Need the proper dynamic for the chemical changes expected

 - Slow measurements at high resolution:
 - Small sample sizes
 - Target specific regions

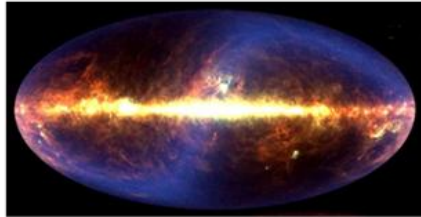
 - Number of samples (Statistical significance, statistical power)

- Provide better sensitivity
 - Unless you can get better sensitivity from measuring at **higher spatial resolution**
- Give narrower absorption bands
 - The absorption band width is caused by the **conformational freedom** of the molecules
 - Absorption bands measured with an IR or a synchrotron source will have the same width
- Penetrate deeper in sample
 - The synchrotron source can not measure thicker samples than conventional sources
 - Absorption obeys the **Beer-Lambert-Bouguer** law for all sources
 - **Near-IR** radiations penetrate 10-100 times deeper than mid-IR in samples
 - But what is the point of having micrometer **lateral** resolution over millimeters in the **axial** direction?

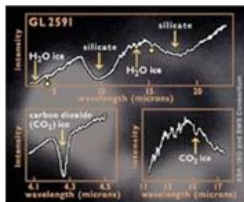


INFRARED SPECTROSCOPY IN SCIENCE & TECH

From parsec
to nm

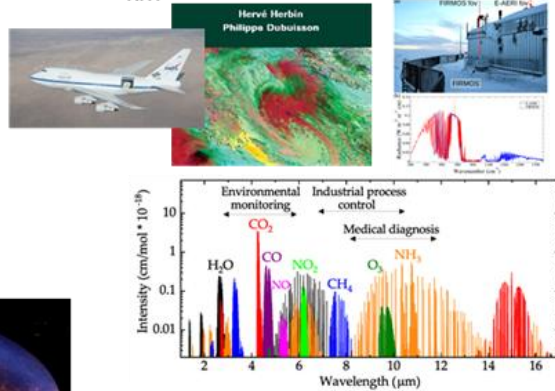


The Infrared Sky
January 28, 1998
DIRBE Team, COBE, NASA



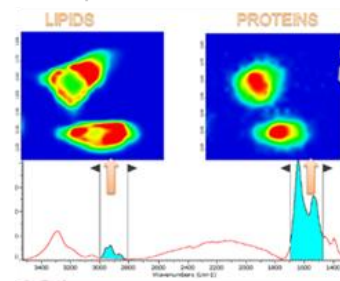
Warm dust ~100 μm
Cool stars energy peak ~1 μm
Giant planets ~6-15 μm
PAH 6 μm , silicates 10 μm
Dust re-radiation ~20-200 μm

Atmospheric analysis
km²

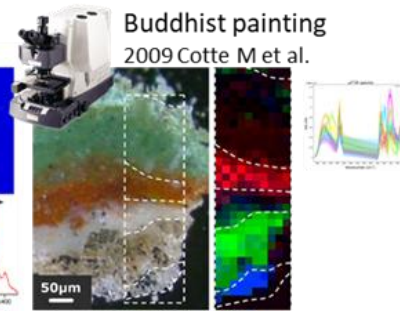


Agilent 4300
Handheld spectrometer
Few mm²

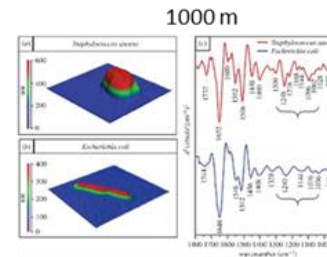
Single HeLa cell
2008 Chio-Srichan S et al.
Few μm^2



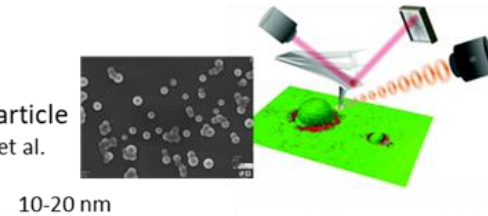
Buddhist painting
2009 Cotte M et al.



Single bacteria
2018 Kochan et al.
Interface



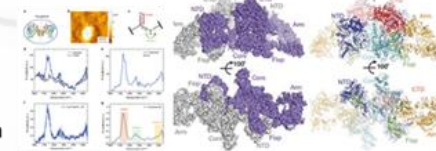
Single nanoparticle
2018 Mathurin et al.
Analyst



10-20 nm

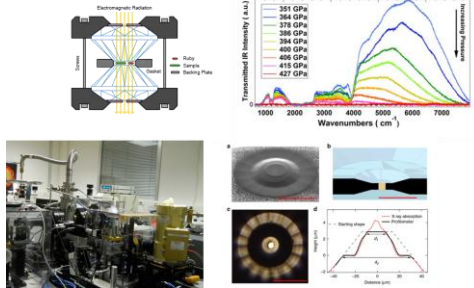
Single protein
2020 Ruggieri et al.
Nature Comm, 11

Few nm

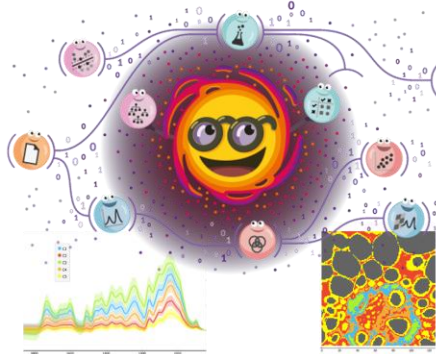


Mid IR spectroscopy
is used across
multiple scales &
sciences

Materials in extreme conditions High Pressure

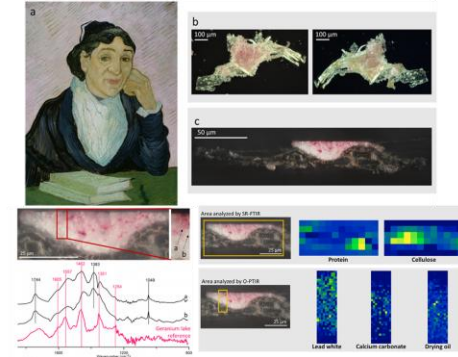


Data analysis

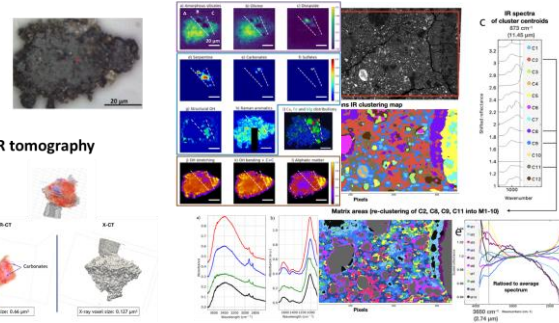


Quasar software
<https://quasar.codes>

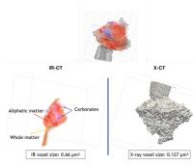
Cultural heritage



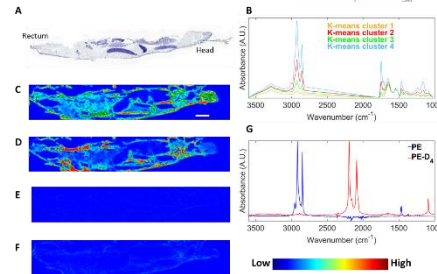
Astrophysics



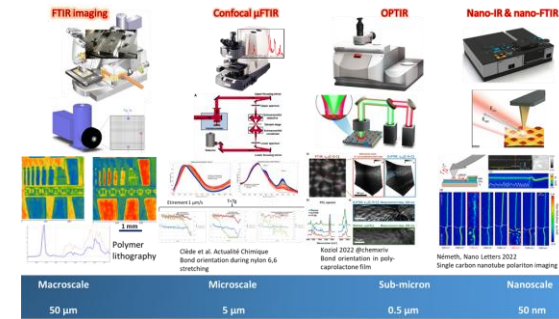
IR tomography



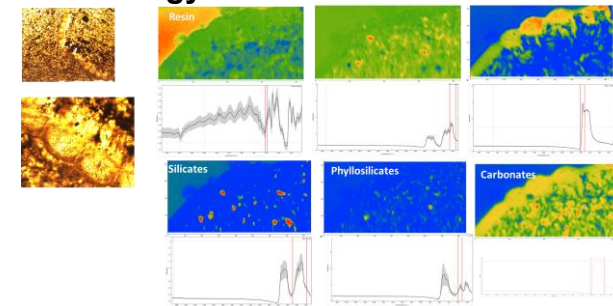
Environnement



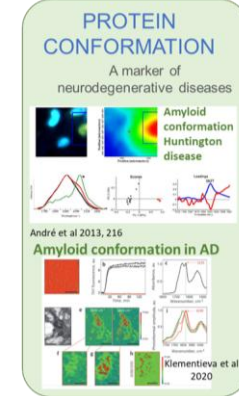
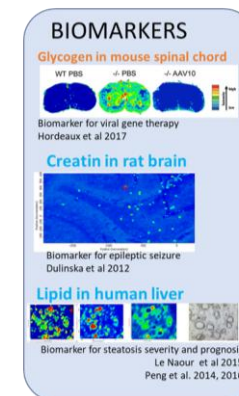
Polymer sciences

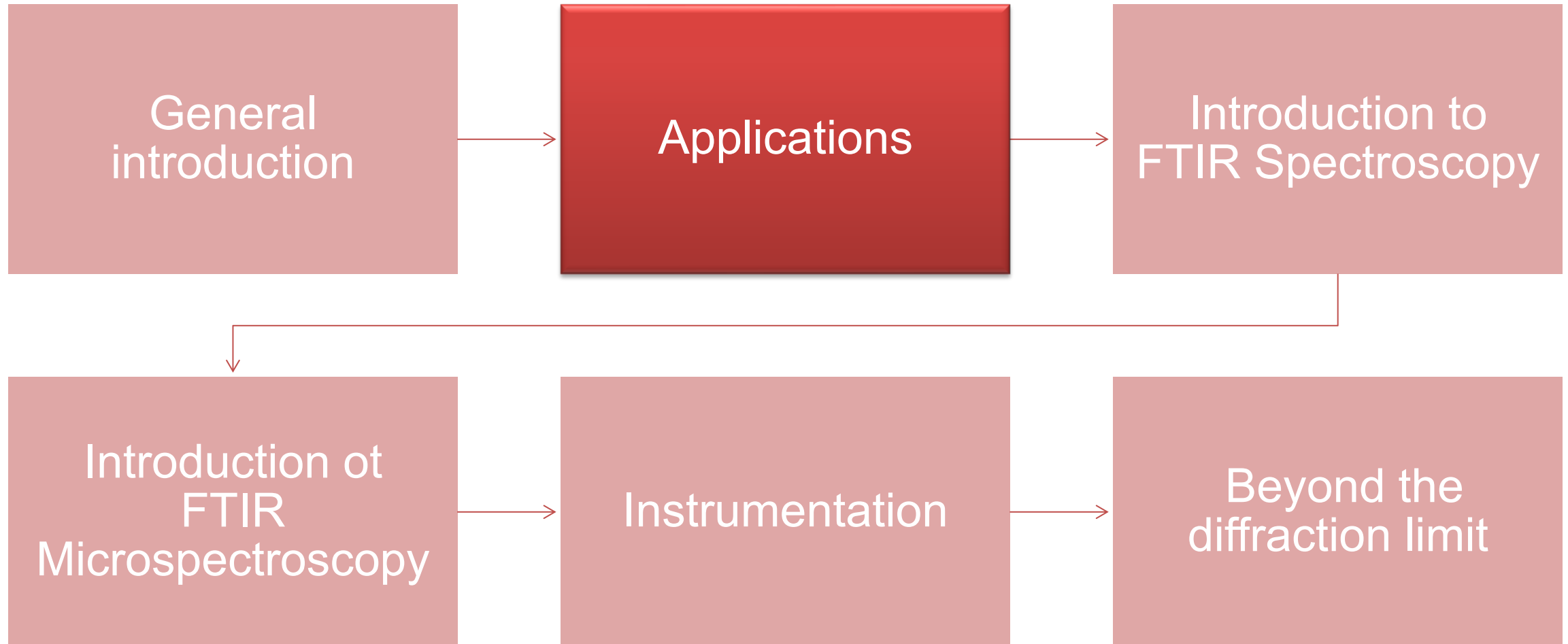


Paleontology

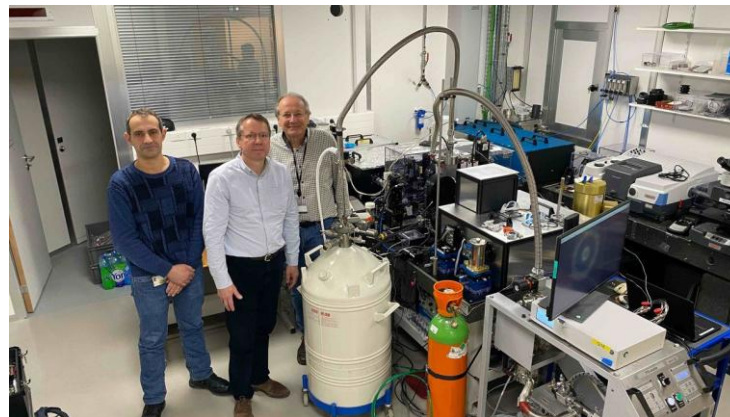


Biology and Biomedical

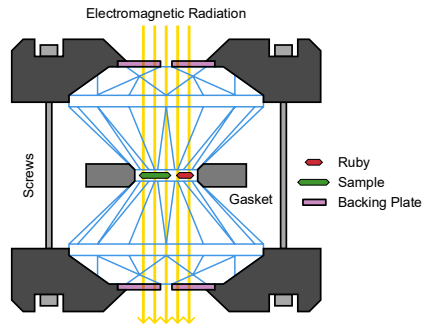




- Most simple gas can turn into metals in the correct Pressure/Temperature conditions
- Hydrogen was the last simple gas that had not been metallized
 - Metal hydrogen predicted in 1935 Wigner, E. & Huntington, H. B. On the possibility of a metallic modification of hydrogen. *J.Chem. Phys.* 3, 764–770 (1935).
 - Five experimentally described phases of hydrogen
 - Phases I, III and IV: isostructural, hexagonal close-packed crystal lattice (300K, 254 Gpa)
 - Phases IV and V exist only above 200 K.
- Transition to metallic hydrogen predicted at 450 GPa (4.5 million atmospheres)



- The tools: Diamond Anvil Cell (DAC)

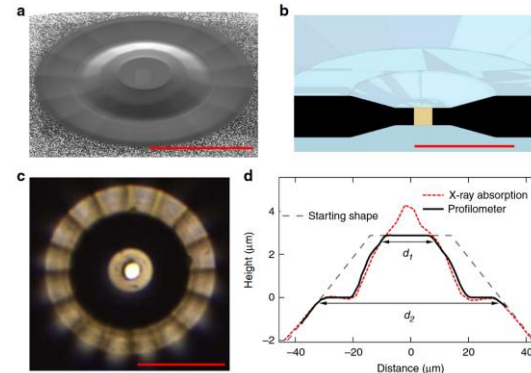


Pneumatic Drive System

– horizontal microscope

Loubeyre, Occelli, Dumas arXiv 2018
Loubeyre, Occelli, Dumas Nature 2020, 577,

Measurements in a DAC inside a cryostat (at 80K) through a micrometric pinhole in a metallic gasket.
Initial pinhole size 10 μm ; final 3-5 μm



Loubeyre, Occelli, Dumas arXiv 2018
Loubeyre, Occelli, Dumas Nature 2020, 577,

Toroidal diamond culet
Pressures up to 600 GPa (6 Mbar)

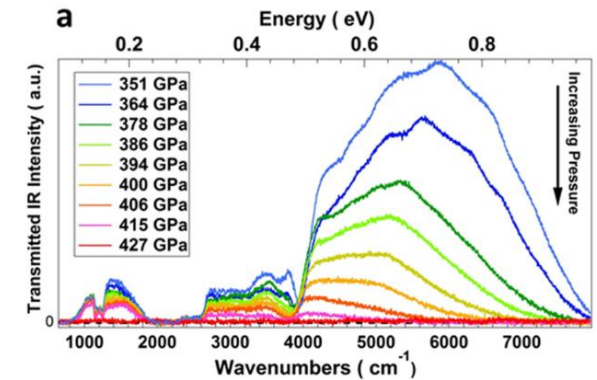
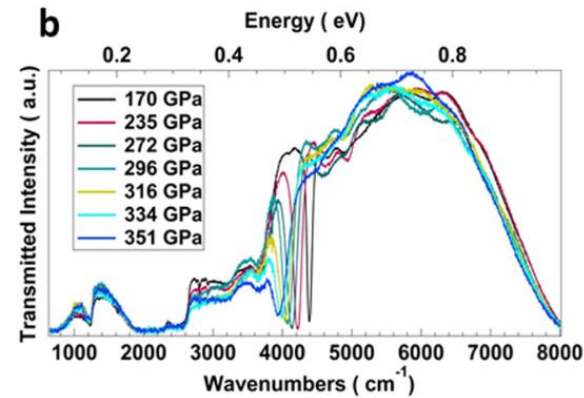
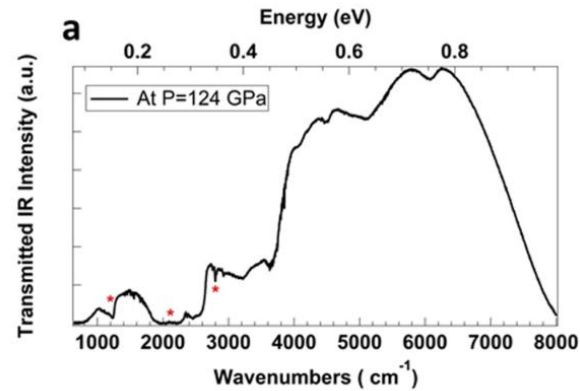
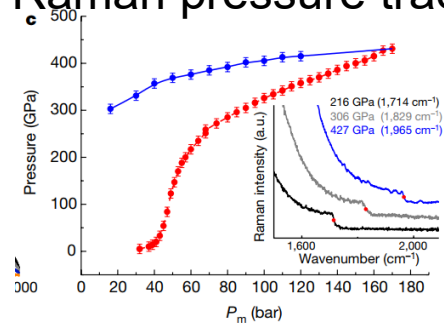


Horizontal microscope
47 mm working distance to accommodate cryostat
15X magnification, 0.5NA
23 μm FWHM IR spot @ 10 μm wavelength

Raman accessory to measure diamond pressure

- Closure of the Fermi bandgap from the visible to the infrared domain

Raman pressure tracking



- Continuous vibron frequency shift
- First order phase transition near **425 GPa/80K** from insulator molecular solid hydrogen to metal hydrogen (4.25Gpa = 4.25 million atmospheres)
- Electronic band gap closure down to 0.5 eV
- Reversible phase transition, back to C2/c-24 phase

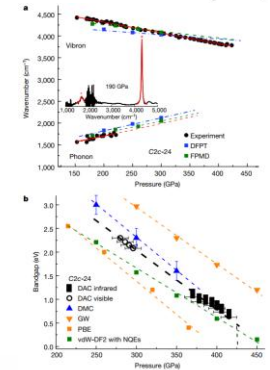
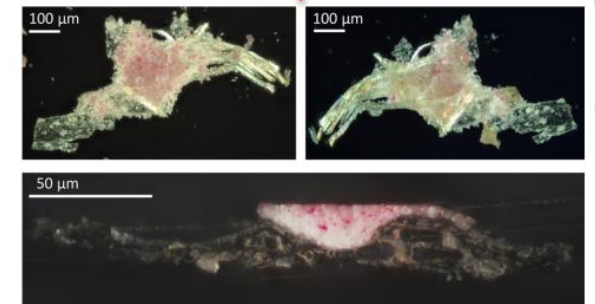


Fig. 3: Evolution of the molecular solid hydrogen properties up to the insulator-metal transition: comparison between experiment and calculation. a. Wavenumbers of the vibron and of the phonon infrared active

- Multiscale characterization of multilayered historical paintings
 - Layers < 10µm
- Non destructive analysis needed
- Ability to identify pigments, binders, support material...
- Characterization of material aging and degradation pathways
- Combination of OPTIR and SR-µFTIR
- Thin sections

L'Arlésienne
Portrait de madame Ginoux,
Van Gogh, 1888
Kröller-Müller Museum,
Netherland



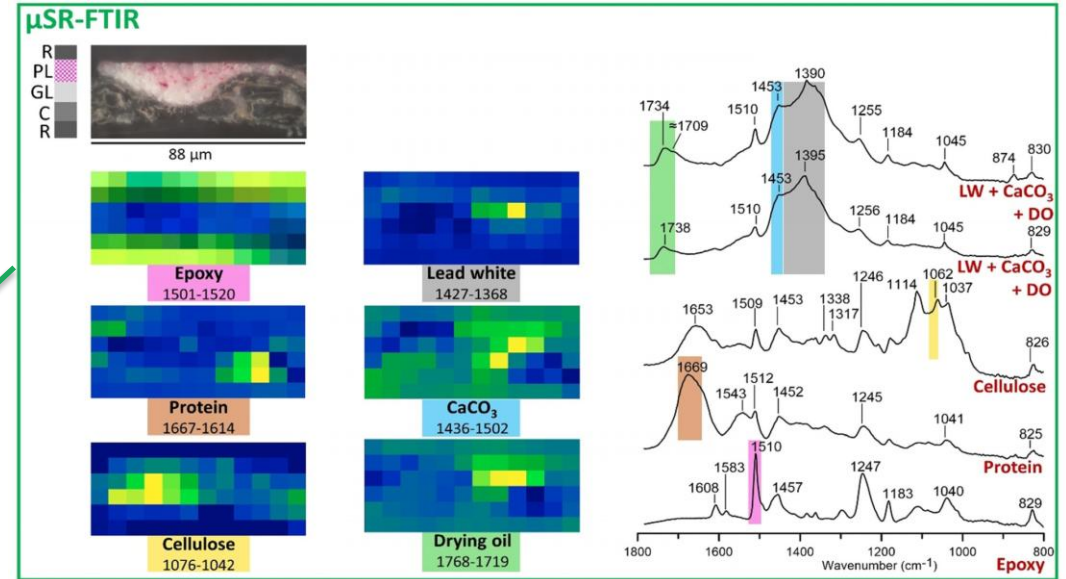
Universiteit
Antwerpen



Beltran V. et al. 2021
Angewandte Chemie

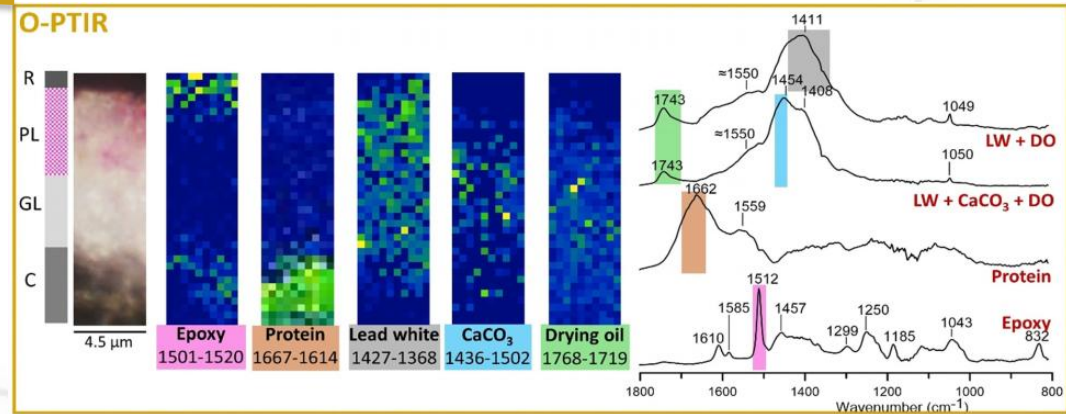
- SR- μ FTIR characterization of:

- Proteins , Calcium carbonate
- Lead white, oil
- Cellulose (canva)
- Epoxy resin



- OPTIR:

- Lead white, oil, CaCO₃
- Proteins and epoxy resin



Measuring the pink pigment in microparticles

- Small pink particles of 2 μm diameter
- Identification of a pink pigment in Raman
 - But possible confusion with other pink pigments
 - Several peaks missing in the Raman spectra
- Confirmation with OPTIR
 - Carboxylates 1550 and 1460 cm^{-1}
 - Xanthene and ketones 1605, 1351, 1254 cm^{-1}
 - Resolved from the oil binder! 1719 cm^{-1}
 - Geranium lake characteristic peaks: 1560, 1465, 1355, 1240 cm^{-1}

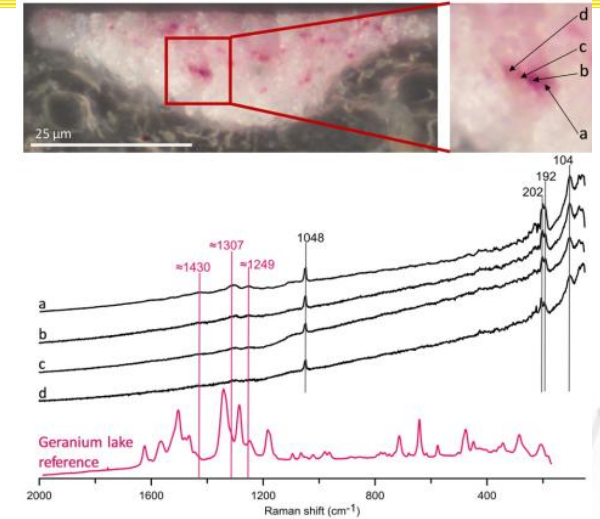


Figure 4. Characterization of a pink particle by μ Raman spectroscopy.

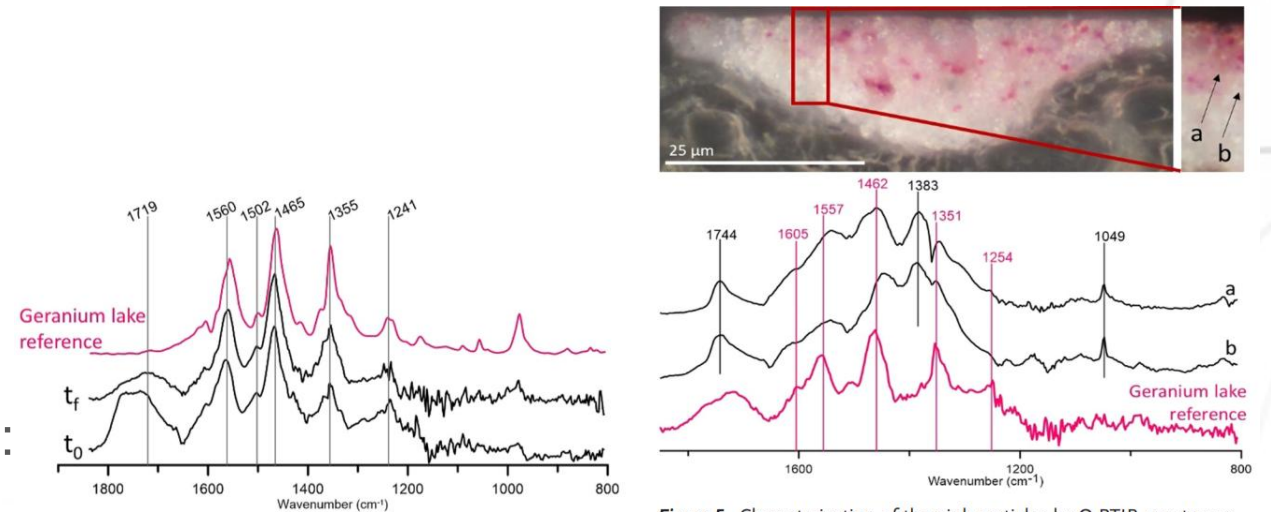


Figure 5. Characterization of the pink particles by O-PTIR spectroscopy.

- First observation of Geranium lake in this painting
- Geranium lakes have been previously observed in other paintings by Van Gogh
 - Normally detected by the presence of Br
 - Br not detected by SEM-EDX here
- GL is photosensitive
 - No photodegradation observed with OPTIR
- OPTIR positively confirmed the presence of geranium lake in this Van Gogh painting

Beltran et al. 2021
Angewandte Chemie

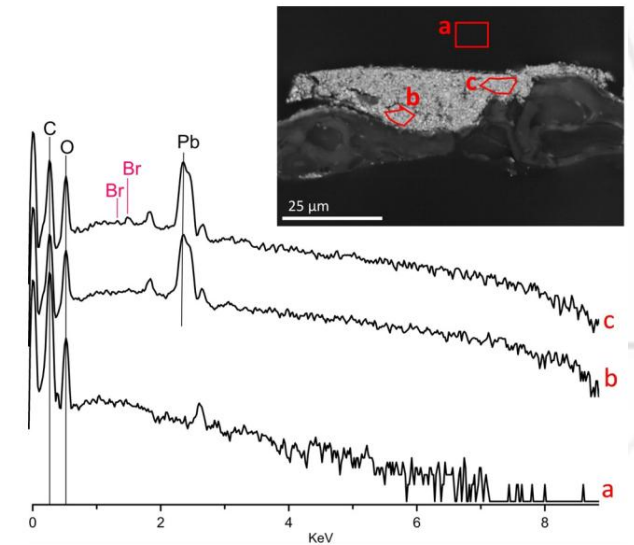


Figure 6. Characterization of the paint layer by SEM-EDX. BSE image



Do *G mellonella* larvae really bioassimilate PE?

ENVIRONMENTAL SCIENCE & TECHNOLOGY

Evidence of Polyethylene Biodegradation by Bacterial Strains from the Guts of Plastic-Eating Waxworms
Jun Yang^{1,2}, Jun Yang¹, Wei-Min Wu¹, Jun Zhou¹, and Lu Jiang¹ | 2015

Biodegradation and Mineralization of Polystyrene by Plastic-Eating Mealworms: Part 1. Chemical and Physical Characterization and Isotopic Tests
Jun Yang^{1,2}, Jun Yang¹, Wei-Min Wu¹, and Lu Jiang¹ | 2015

Biodegradation and Mineralization of Polystyrene by Plastic-Eating Mealworms: Part 2. Role of Gut Microorganisms
Jun Yang^{1,2}, Jun Yang¹, Wei-Min Wu¹, Jun Zhou¹, Yiling Long¹, Luyang Gong¹, Huiyi Yang¹, and Lu Jiang¹ | 2015



T. molitor larvae eating polystyrene
Yang et al, ES&T 2015

Galleria mellonella (Gm) | Current Biology Magazine

Correspondence Polyethylene bio-degradation by the wax moth *Galleria mellonella*
Paolo Bombelli¹, Christopher J. Howe^{1,2}, and Federica Bertocchini^{1,2,3,4} | 2017

Plastics are synthetic polymers derived from fossil oil and largely resistant to biodegradation. Polyethylene (PE) and polypropylene (PP) represent ~92% of total plastic production. PE is largely utilized in packaging, representing ~40% of total demand for plastic products (www.plasticseurope.org) with over a trillion plastic bags used every year [1]. Plastic production has increased exponentially in the past 50 years (Figure S1A in Supplemental Information, published with this article online). In the 27 EU countries plus Norway and Switzerland up to 38% of plastic is discarded in landfills, with the rest utilized for recycling (26%) and energy recovery (36%) via combustion (www.plasticseurope.org), carrying a heavy environmental impact. Therefore, new solutions for plastic degradation are urgently needed. We report the first biodegradation of PE by larvae of the wax moth *Galleria mellonella*, producing ethylene glycol.

PROCEEDINGS B | Role of the intestinal microbiome in low-density polyethylene degradation by caterpillar larvae of the greater wax moth, *Galleria mellonella*

Research
On this article: Laura S. Lee, Sean K. O'Leary, E. William Sill, Jeffrey D. R. Hill, and J. R. Powell | 2017

Science of the Total Environment
Journal homepage: www.elsevier.com/locate/scitotenv

Technological application potential of polyethylene and polystyrene biodegradation by macro-organisms such as mealworms and wax moth larvae
Peter Billen^{1,2}, Liana Khalifa¹, Femio Van Geven¹, Serge Tavernier¹, Sabrina Spatari¹

International Journal of Environmental Research and Public Health | MDP

Biodegradation of Polyethylene by *Enterobacter* sp. D1 from the Guts of Wax Moth *Galleria mellonella*
Liu Ren^{1,2}, Lina Men², Zhiwei Zhang², Feifei Guan², Jian Tian^{2,3}, Bin Wang^{1,4}, Jihua Wang^{1,4}, Yuhong Zhang^{1,2,3} and Wei Zhang²



CellPress | Current Biology Magazine

Correspondence Polyethylene bio-degradation of the wax moth *Galleria mellonella*
Paolo Bombelli¹, Christopher J. Howe^{1,2}, and Federica Bertocchini^{1,2,3,4}

Plastics are synthetic polymers derived from fossil oil and largely resistant to biodegradation. Polyethylene (PE) and polypropylene (PP) represent ~92% of total plastic production. PE is largely utilized in packaging, representing ~40% of total demand for plastic products (www.plasticseurope.org) with over a trillion plastic bags used every year [1]. Plastic production has increased exponentially in the past 50 years (Figure S1A in Supplemental Information, published with this article online). In the 27 EU countries plus Norway and Switzerland up to 38% of plastic is discarded in landfills, with the rest utilized for recycling (26%) and energy recovery (36%) via combustion (www.plasticseurope.org), carrying a heavy environmental impact. Therefore, new solutions for plastic degradation are urgently needed. We report the first biodegradation of PE by larvae of the wax moth *Galleria mellonella*, producing ethylene glycol.

Figure 1. Polyethylene degradation by *Galleria mellonella*.
(A) Plastic bag after exposure to ~100 wax worms for 12 hours. (B) Magnification of the area indicated in A. (C) Gravimetric analysis of homogenate-treated versus untreated polyethylene (PE), showing a reduction (13%) of mass per unit of area in the former. (D,E) FTIR analysis of the homogenate-treated and control PE films. (F,G) Atomic Force Microscopy on homogenate-treated (F) and untreated (G) PE film (representative examples of 3 topographic maps each).

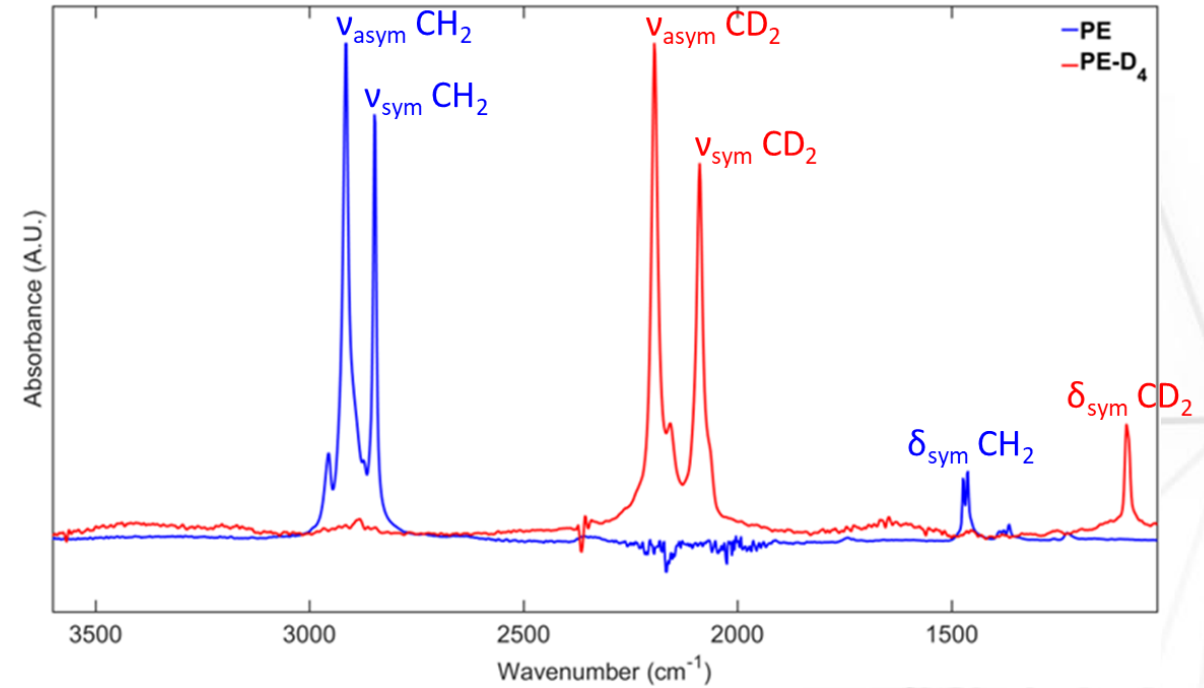
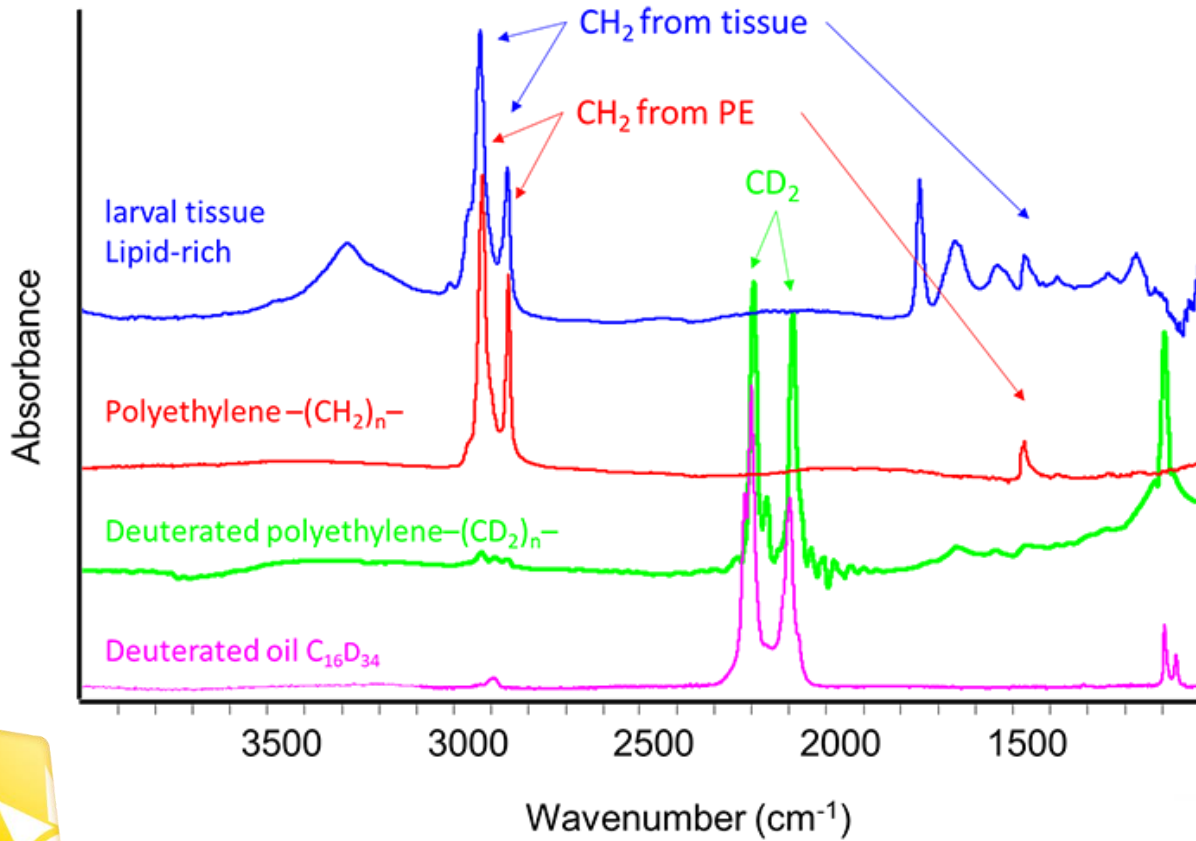
Correspondence Polyethylene bio-degradation by caterpillars?

Carina Weber, Stefan Pusch, and Till Opatz*

CO from lipid esters. Not from PE oxidation

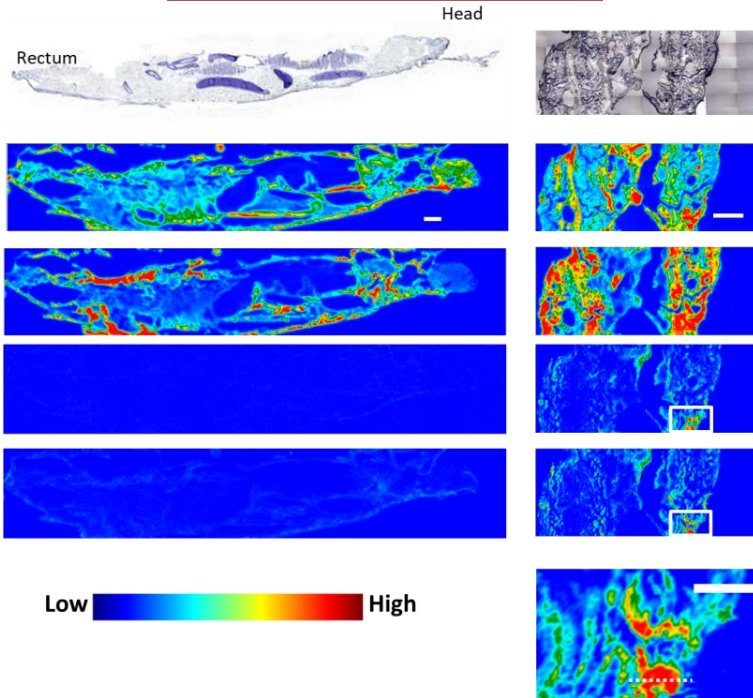
C=O from protein peptide bonds. Not from PE oxidation

Do *G mellonella* larvae bioassimilate PE?

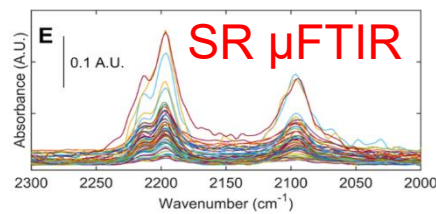
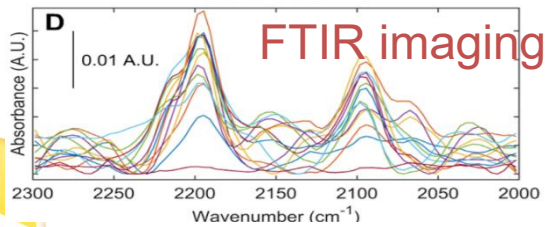
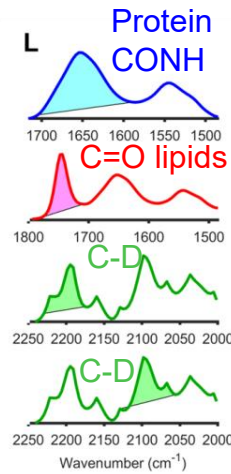


Do *G mellonella* larvae bioassimilate PE?

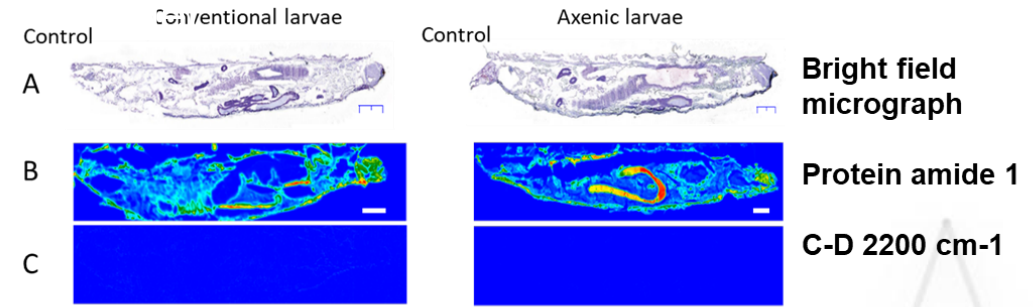
Deuterated oil diet



Réjasse et al. ES&T
2022

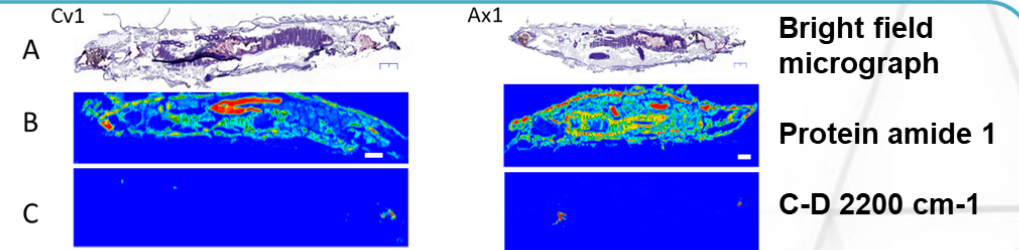


Deuterated PE

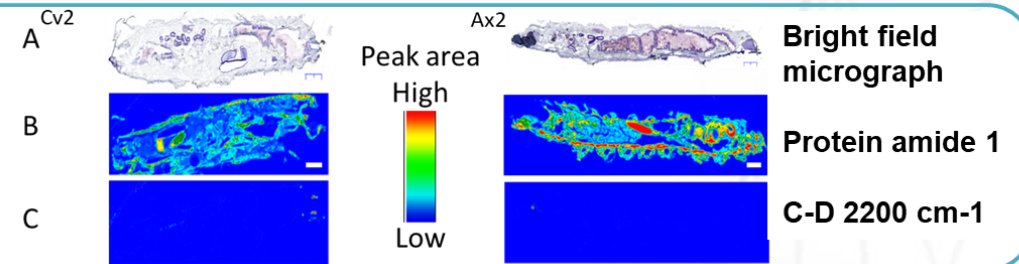


PED4 consumption

2.1 mg in 72h



3.7mg in 19 days
(alternating diet)



Do *G mellonella* larvae bioassimilate PE?

- Deuterium can be detected in larvae fed with deuterated oil

- Discrete location after 24h
- In all fat tissues after 72h

Isotopic labelling food with deuterium can be used to follow bioassimilation of 1-2 mg of food

- *G mellonella* larvae do not assimilate PE

- Young larvae (L3 stage) die after 3 days on a PE diet
- Old larvae (L6 stage) survive but stop gaining weight
- No deuterium is found in larvae after a deuterated PE diet

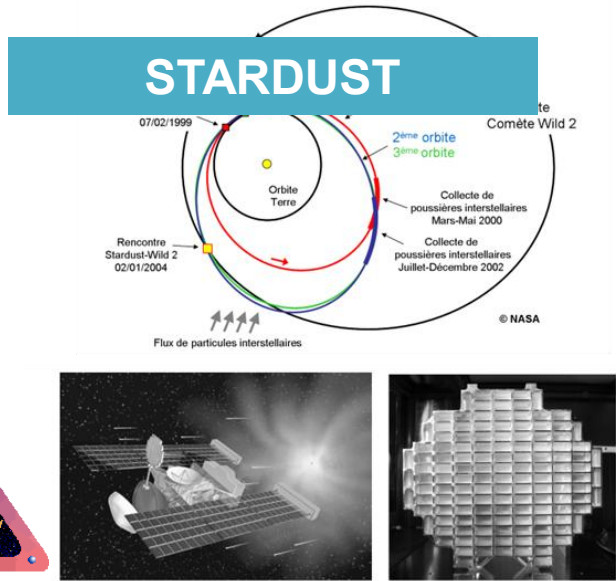
PE is not transformed into biomass by the larvae

- *G mellonella* chew PE

- PE is fragmented in micro/nanoplastics
- PE fragments travel in the larvae gut
- PE fragments are excreted in the frass
- PE is weakly oxidised in the process

Larvae create minuscule fragments that are more difficult to collect and eliminate

- Everything we know about the solar system and other galaxies is from telescopic spectroscopy observations
 - IR observatories, satellites (IRAS, COBE, Spitzer, HERSCHEL)
- Laboratory analyses are necessary to understand these observations
 - IR microspectroscopy is widely used for organic and inorganic matter characterization
 - Laboratory Analogs and Sample return mission
- Results answers questions about:
 - The composition of planets, asteroids, stars, dust, clouds and nebula...
 - The evolution of the solar system
 - The origin of water, inorganic and organic molecules on earth



STARDUST

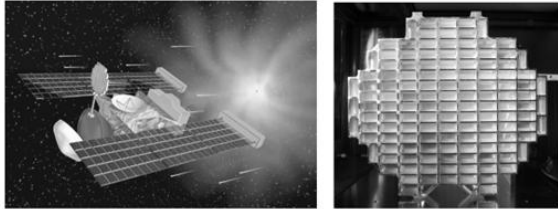
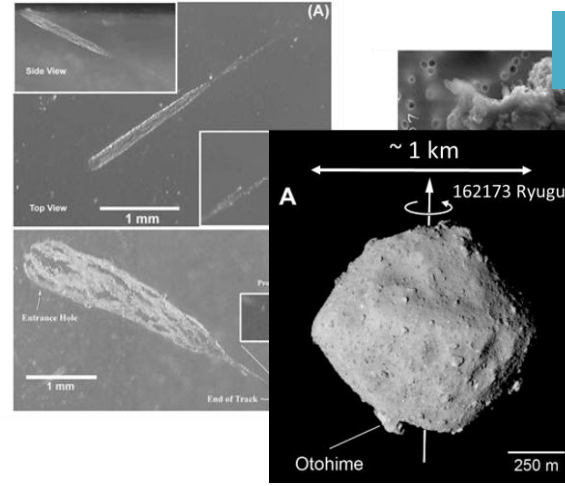


Figure 1.1 – Image optique de la trace 35 extraite de la cellule C2054. La flèche indique la région où ont été prélevées les particules 35,21 et 35,26. ©NASA.

OSIRIS REX

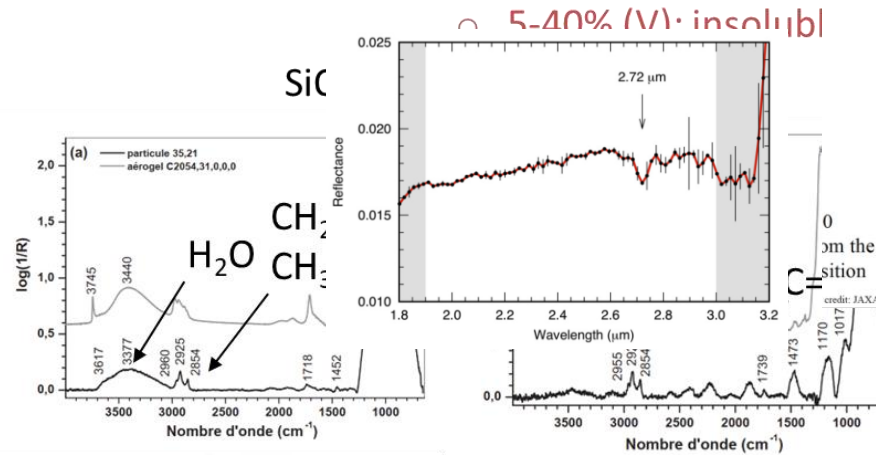
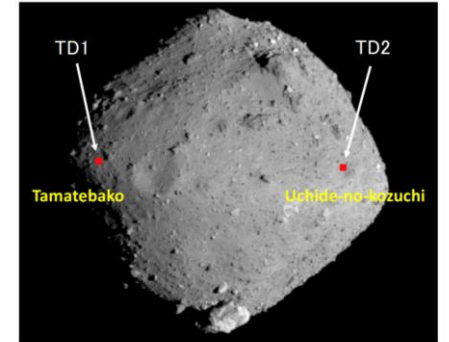


Hayabusa 2



Albedo	0.045 +/- 0.002	0.044 +/- 0.002
Spectral Type (Tholen taxonomy)	C	B
Density	~1.19 g/cm ³	~1.26 g/cm ³

Locations for the 1st (TD1) and 2nd (TD2) touchdown
 me. crystalline forsterite



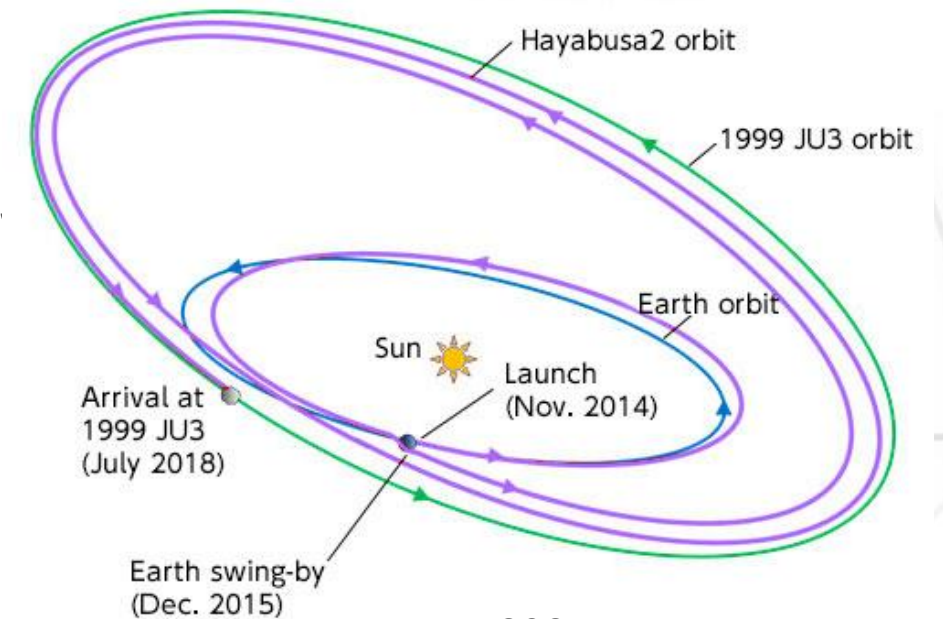
F Grossemy, PhD thesis 2008





- **November 30, 2014: Launch**
- **End of 2015: Earth swing-by**
- **Summer 2018: Arrival at the asteroid**
 - Stay there for about 18 months
 - IR observation: Near InfraRed Spectrometer (NIR) and the Thermal Infrared Imager (TIR)
 - Separating the small rover “MINERVA”
 - Separating the small lander “MASCOT”
 - Sample collection
 - Launching the Small Carry on Impact
- **End of 2020: Return to Earth**

Earth -Ryugu distance : 299,947,616 km
16 minutes 40 sec light travel

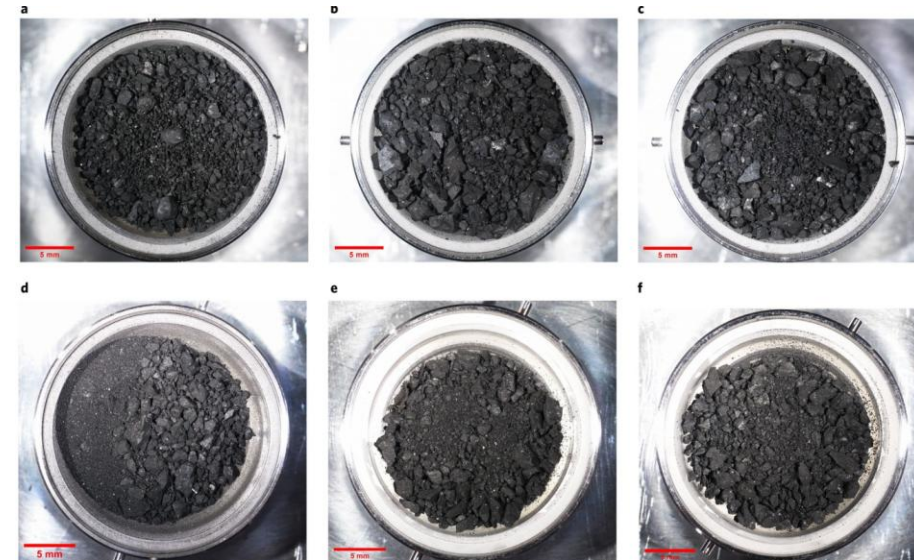


MASCOT Lander

1. MicroOmega infrared microscope
2. Magnetometer (MAG)
3. Radiometer (MARA)
4. Wide-angle camera (CAM)



- Several grams of asteroid matter brought back to earth
- Stored at curation facility in Japan
- Dissiminated to research groups abroad:
 - IAS: Institut d'Astrophysique Spatiale, Orsay
 - ISMO: Institut des Sciences Moléculaires d'Orsay



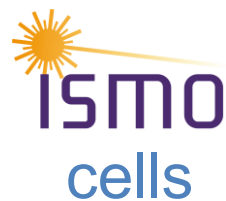
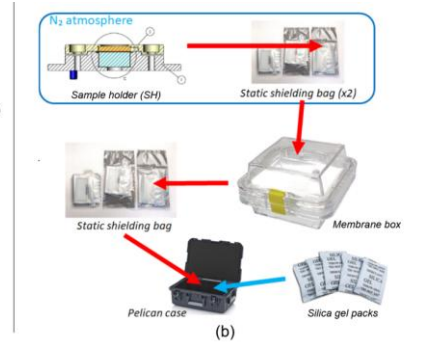
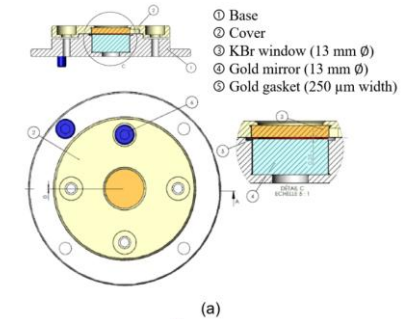
Optical microscopic images of bulk samples from Chambers A and C

2 radically different strategies



IAS: try to preserve the grains from atmospheric alterations

- Synchrotron μ FTIR and μ Raman of whole grains
- IR tomography
- MicrOmega instrument on board the lander and at curation facility



ISMO: flatten the grains in Diamond Compression cells

- Synchrotron μ FTIR: mid-IR and far-IR
- AFM-IR

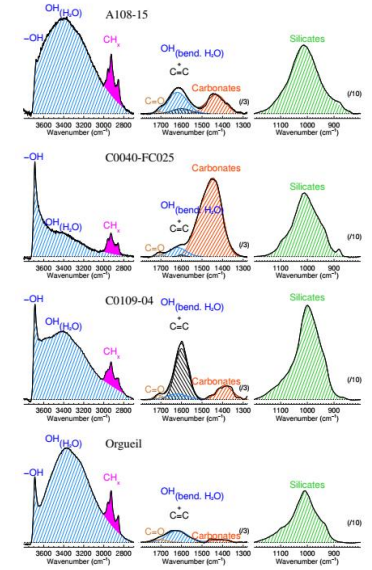
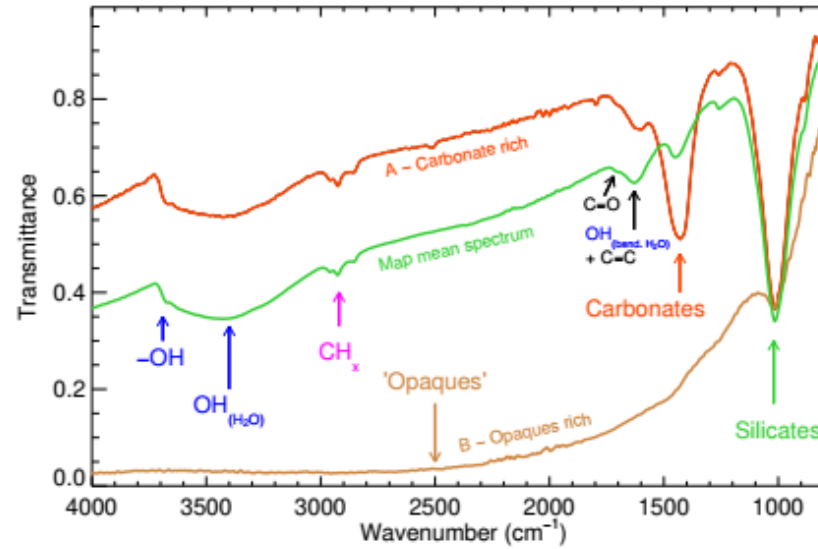


• SR- μ FTIR

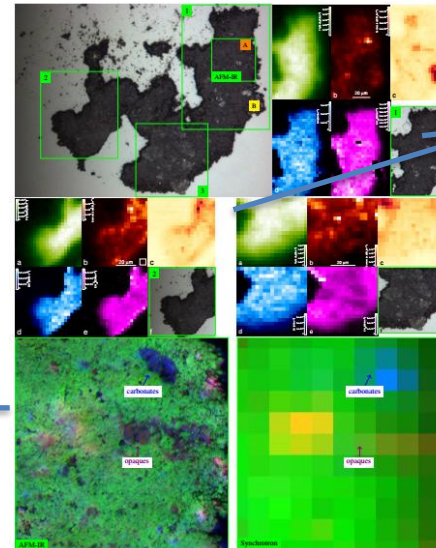
- Phyllosilicate matrix
- Organic component dominated by aliphatic CH_x , high CH_2/CH_3 ratio
- C=C ubiquitous
- Carbonates : dominated by dolomite and saponite (far-IR)
- Very similar composition to other carbone rich meteorites

• AFM-IR

AFM-IR map
Silicate
Carbonates
"Opagues"

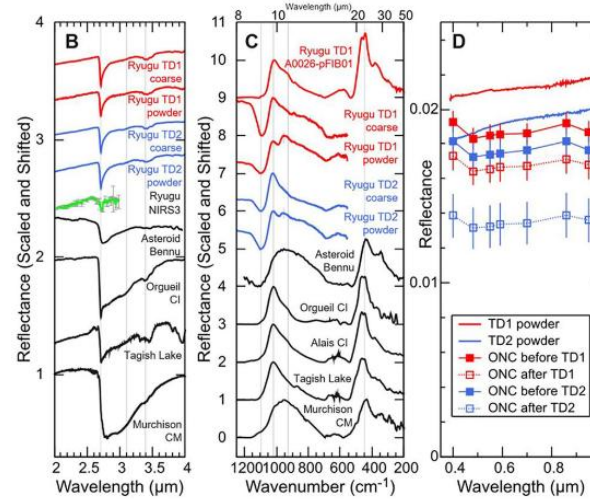
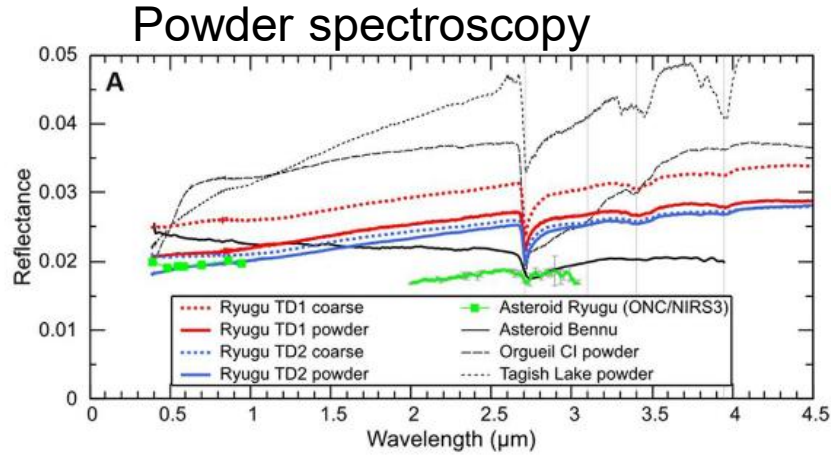


150 μ m

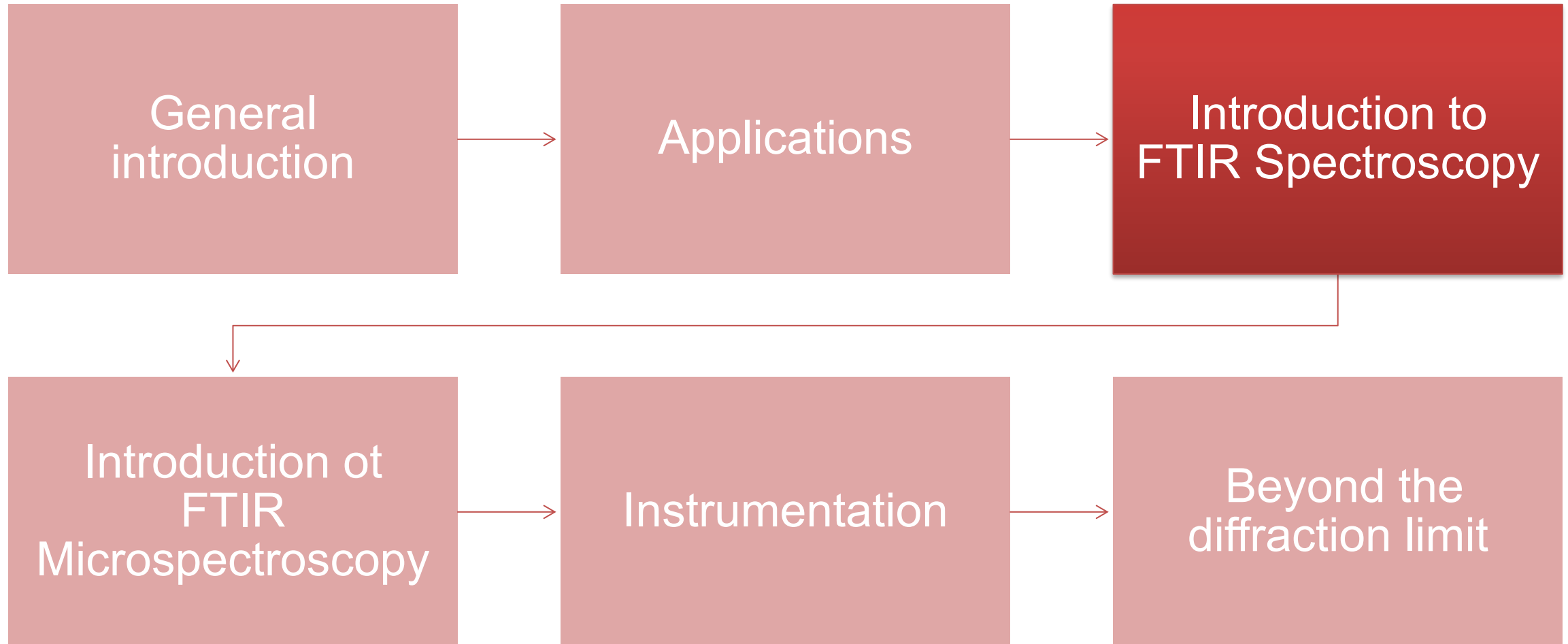


SR- μ FTIR maps
Silicate
Carbonates
"Opagues"

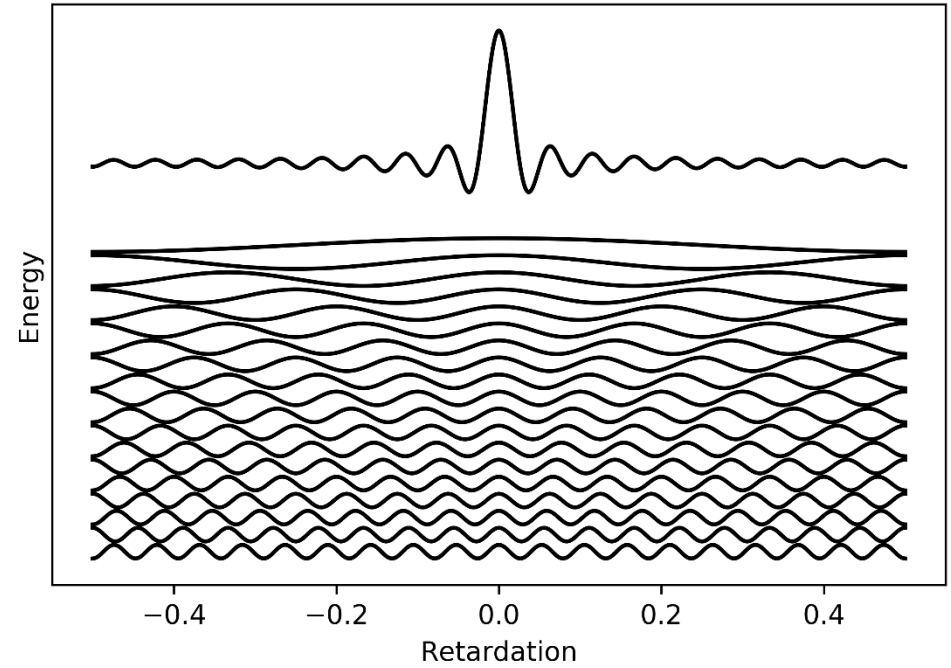
Single grain microspectroscopy



- Ryugu is similar to known CIs with important differences
- Ryugu is very close to Orgueil meteorite
Existing meteorite collection is biased!
- Ryugu is the new standard for CI
- Ryugu has formed in the far outer system after 2 My and then migrated closer to the sun
- Rich in silicates and carbonates
- 3 My at 50°C: aqueous alterations
- Traces of olivine, pyroxene, amorphous silicates, calcite, and phosphide



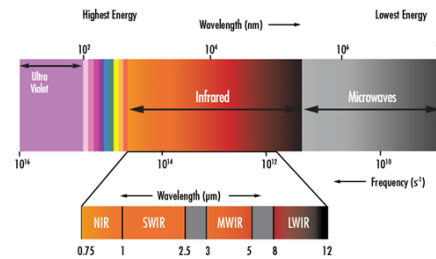
FT-IR SPECTROSCOPY



Optical method in the IR range

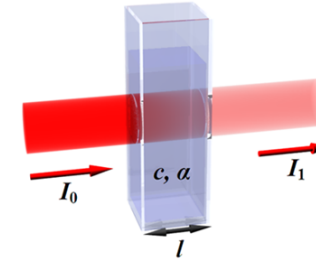
- "Light*" - matter interaction
- Near, mid, far IR:

* actually IR radiation, not light



Domain	Wavelengths	Wavenumbers
Near IR	0.8-2.5 μm	1250 – 4000 cm ⁻¹
Mid IR:	2.5-25 μm	4000 – 400 cm ⁻¹
Far IR	25-1000 μm	400-10 cm ⁻¹ .

Absorption spectroscopy



$$A = -\log \frac{I}{I_0} = \epsilon_{\lambda} c l$$

Beer Lambert Bouguer law

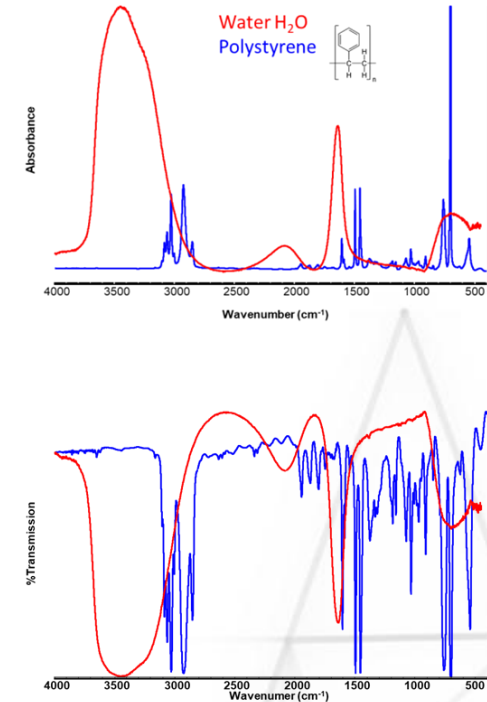
A= Absorbance

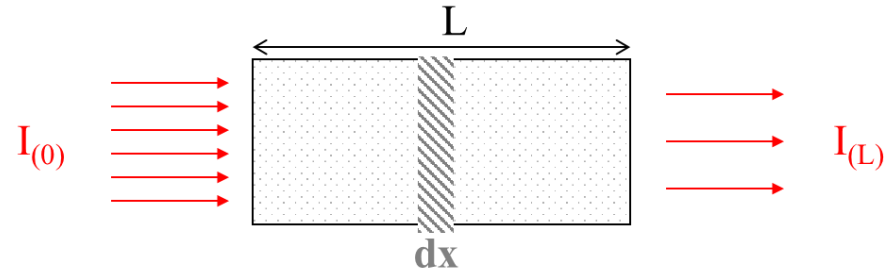
I, I_0 : Intensity of the transmitted and incident beam

ϵ = molar absorptivity (cm⁻¹·L·mol⁻¹)

C= concentration (mol.L⁻¹)

l= pathlength (cm)





$$-dI_{(x)} = KI_{(x)}cdx$$

$$-\left[\ln I(x)\right]_{I(0)}^{I(L)} = [Kcx]_0^L$$

$$\ln\left(\frac{I(0)}{I(L)}\right) = KcL$$

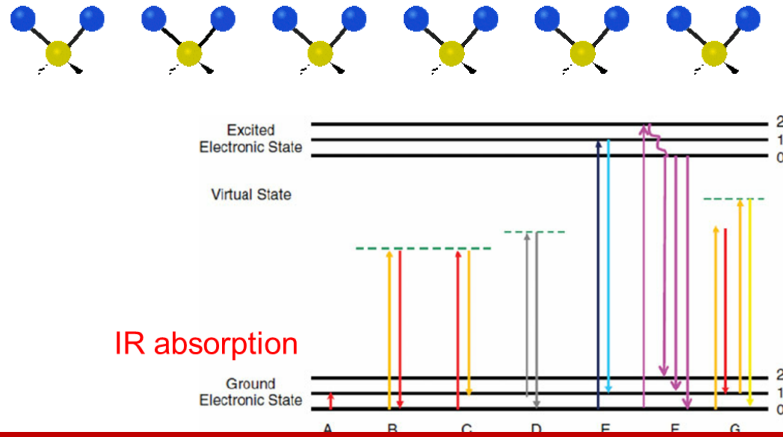
$$\frac{I(L)}{I(0)} = e^{-KcL}$$

$$A = \log\left(\frac{I(0)}{I(L)}\right)$$

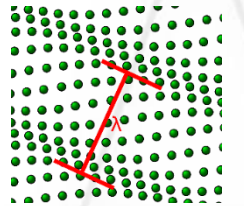
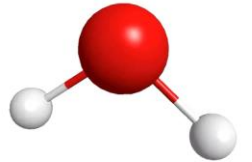
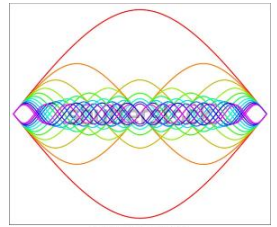
K: absorptivity coefficient
 c: concentration
 x: distance
 I_0 : incident beam Intensity
 I_L : transmitted beam Intensity

VIBRATIONAL SPECTROSCOPY

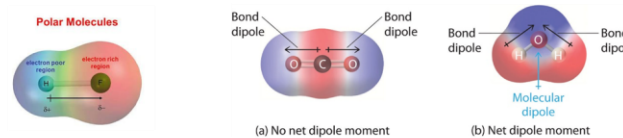
- Probes vibrations of molecular bonds
 - Actually **Ro**vibrational: probes **vibrations and rotations**
 - Rotational** energy levels can only be measured in diluted gas



- Different energy ranges probe different vibration types:
 - Near IR:** 0.8-2.5 μm or 12500 – 4000 cm^{-1} : overtones of fundamental vibrations.
 - Low absorptivity, low sensitivity long penetration pathlength.
 - Mid IR:** 2.5-25 μm or 4000 – 400 cm^{-1} : fundamental vibrations and combinations.
 - High molar absorptivities, high sensitivity, low penetration.
 - Far IR:** 25-1000 μm or 400-10 cm^{-1} : low-energy modes, skeletal vibrations, phonons.



- IR active vibrations: molecular bond with **permanent** dipolar moment



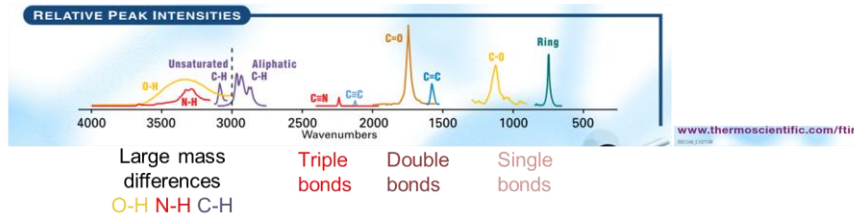
- IR absorption is proportional to the strength of the dipolar moment
- Symmetric bonds/molecules are not active
 - IR spectroscopy is linked to molecular symmetry
 - C-C and C=C bonds are almost inactive
 - Small distortions of the molecule symmetry can make these bonds slightly active

DEPENDENCE ON BOND STRENGTH

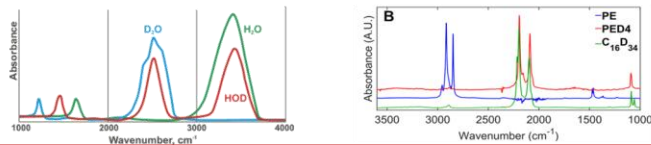
- Peak position depends on bond strength
 - Atom masses and bond conformation
 - Single/double/triple bond

$$\sigma = \frac{1}{2\pi c} \sqrt{\frac{k}{\mu}}$$

In the harmonic approximation

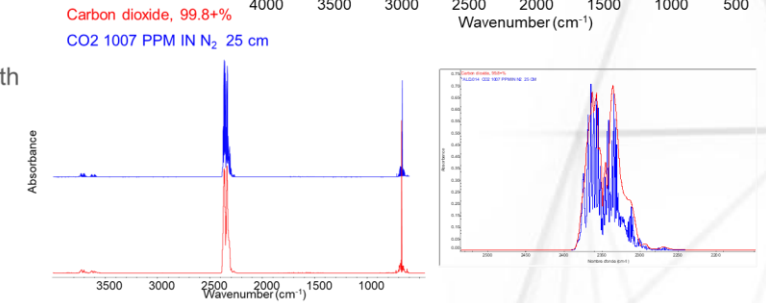
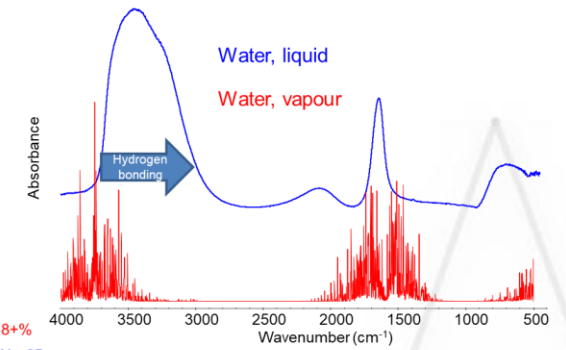


- Isotopic labelling can be used to shift peaks



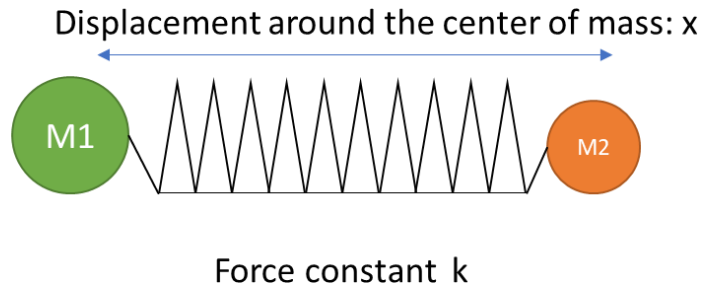
PHASE SENSITIVITY

- Peak width depends on the organisation/phase:
 - Gaz: narrow peaks
- Conformational entropy
 - Crystalline samples: narrow peaks
 - Amorphous samples : large peaks
- Hydrogen - bonding
 - Shift peaks to lower frequency
 - Increases peak width
- Interaction between molecules
 - Affect peak position and peak width



DERIVATION OF THE PEAK POSITION IN THE HARMONIC APPROXIMATION

Vibration frequency f



There is two ways of calculating f :

- Solve the derivative of E_0 versus time which is equal to zero since E_0 is conserved
- Or solve $ma = -kx$

Total Energy:
 $E_c = 1/2mv^2$
 $E_0 = 1/2mv^2 + kx$

$$\vec{F} = -kx$$

$$\vec{F} = m\vec{a}$$

$$E_0 = E_c + E_p$$

$$E_p = kx$$

$$E_0 \text{ is conserved: } \frac{\partial E_0}{\partial t} = 0$$

a : acceleration
 E_0 : total energy
 E_c : kinetic energy
 E_p : potential energy

$$m\vec{a} = -kx$$

$$m \frac{\partial^2 x}{\partial t^2} + kx = 0$$

Solution of the differential equation:

$$x(t) = A \cos(\omega t)$$

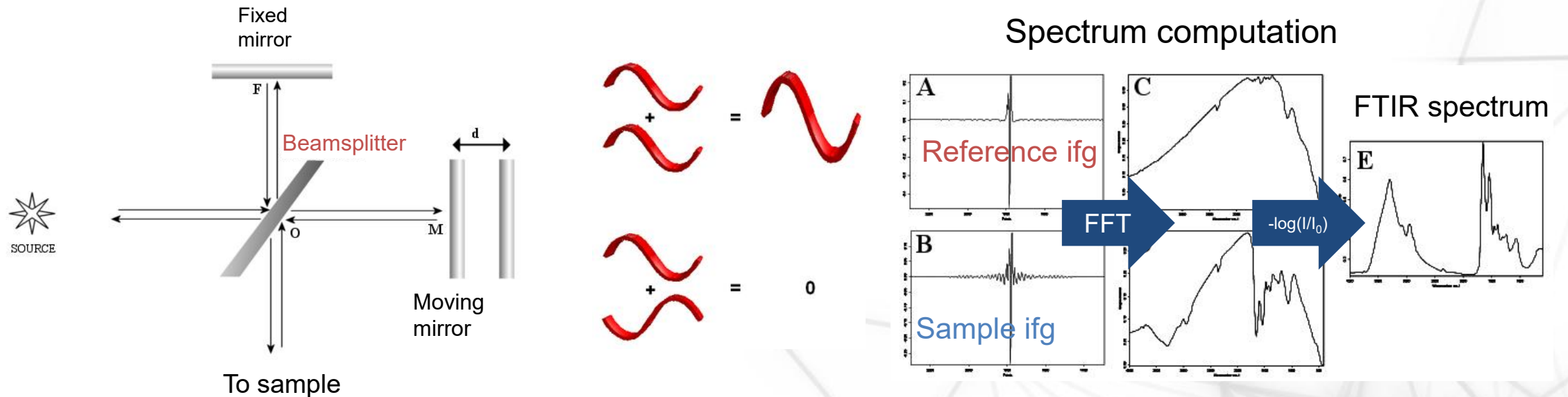
with ω the angular frequency: $\omega = 2\pi f$ with f the oscillation frequency

$$f = \frac{1}{2\pi} \sqrt{\frac{k}{\mu}}$$

K : force constant
 μ : reduced mass

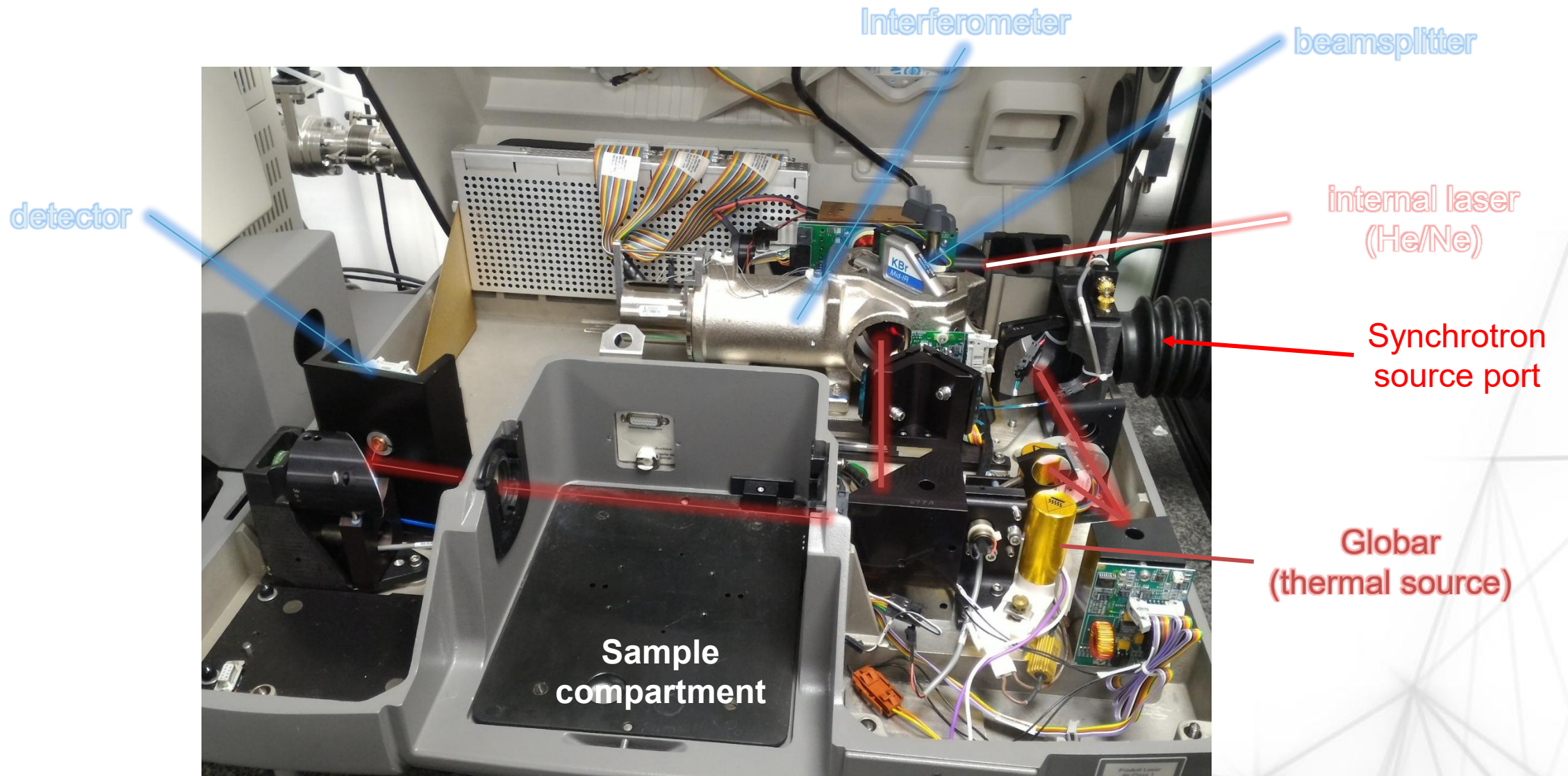
$$\mu = \frac{M_1 M_2}{M_1 + M_2}$$

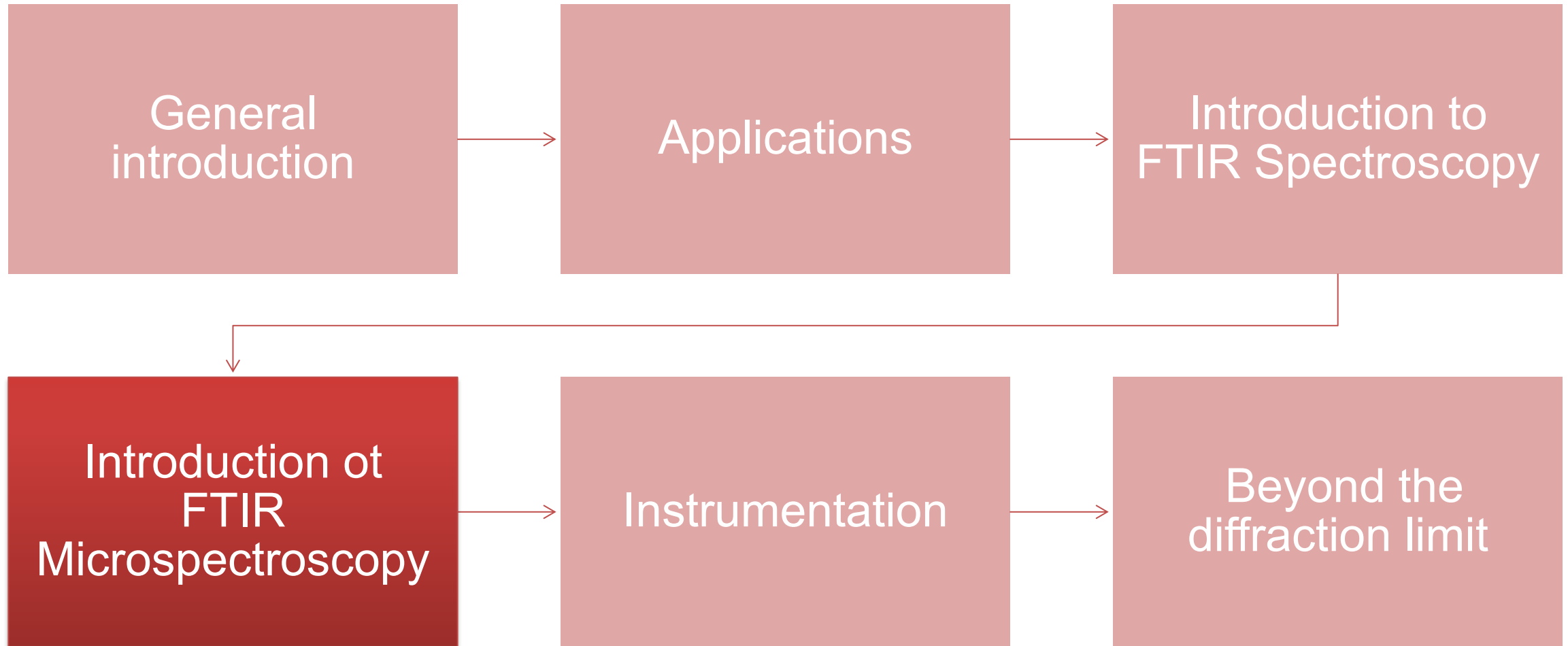
- Most modern IR spectrometers are **Fourier-Transform** spectrometers
- They use an **interferometer** to create **interferences** in the beam
 - The interferometer produces an **interferogram** (ifg)
- **Fast Fourier-Transform (FFT)** is the mathematical operation used to retrieve the wavelengths and compute the single beam spectra
 - Single beam spectra are ratioed to get the final transmittance/absorbance spectrum



- FREQUENCY ACCURACY (CONNE'S ADVANTAGE)
 - Internal laser measuring the mirror position
 - Internal frequency calibration (10^{-4} cm⁻¹)
 - Permanent autoalignment: no need for frequency calibration
- MULTIPLEX ADVANTAGE (FELGETT'S ADVANTAGE)
 - Improvement in signal to noise ratio coming from measuring ALL wavelengths simultaneously (no detector slit or pupils)
- SPEED ADVANTAGE
 - All wavelengths are measured simultaneously: faster measurement
- SIGNAL to NOISE (SNR) advantage
 - Since measurement is faster and accurate it is possible to **average** multiple measurements
 - SNR increases like \sqrt{N} where N= number of scans

ANATOMY OF THE SPECTROMETER



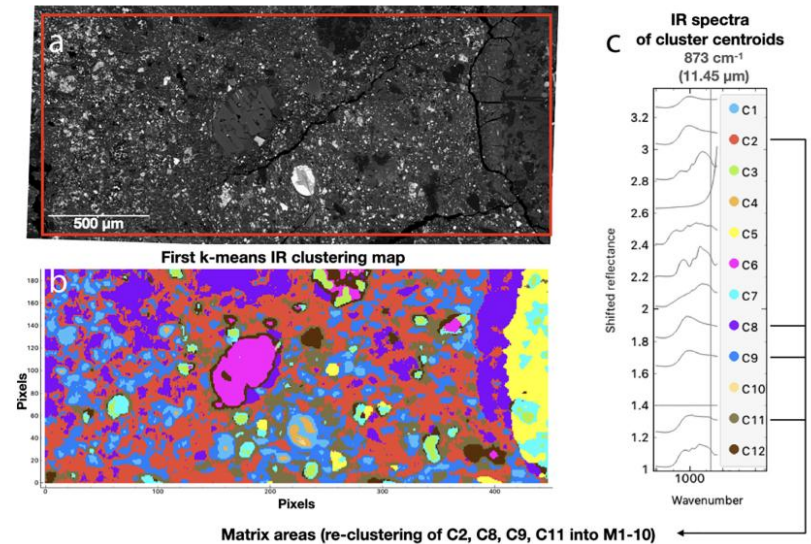


μFTIR results from coupling an FTIR spectrometer and an IR microscope

- Designed to analyze ‘small’ samples
- Multiple commercial solution exist (~60-300 k€)
- Can be used with multiple IR sources
 - Thermal sources (“globalar”)
 - Synchrotron sources
 - Laser sources
 - QCL, SC, OPO...

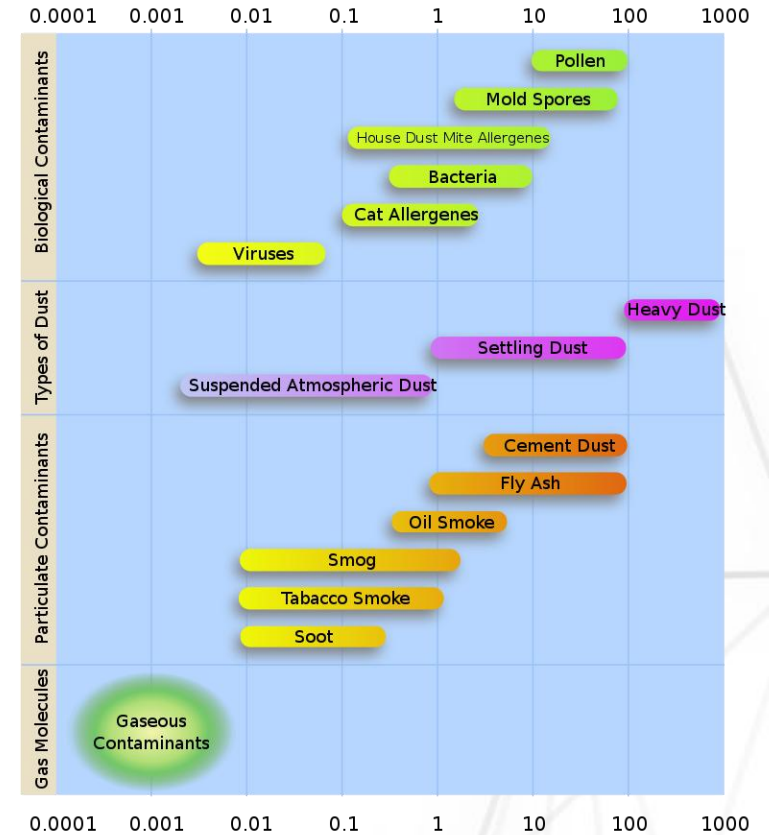
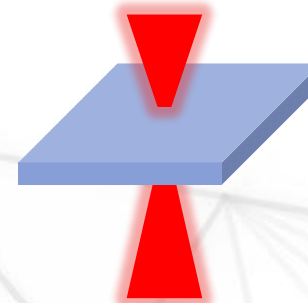
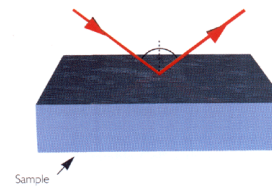


- Measure **small & heterogeneous** samples
- Combine **chemical & spatial** information
- **Chemical mapping**
 - Point by point acquisition of spectra
- **Chemical imaging**
 - Hyperspectral wide field acquisition on large array detectors
 - Single wavelength images

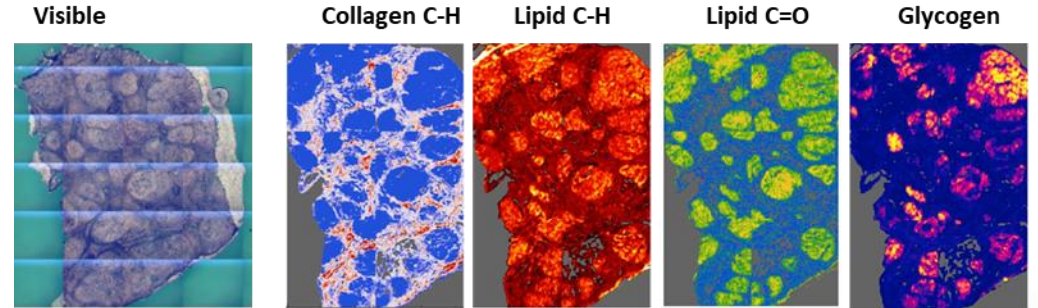


Hyperspectral FTIR imaging of an asteroid thin section
From Hewins et al. 2021

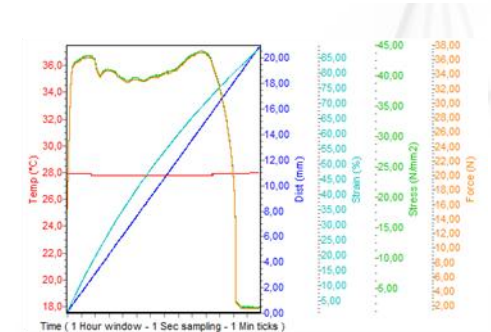
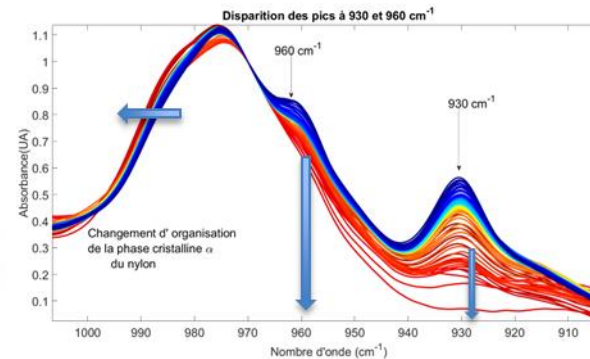
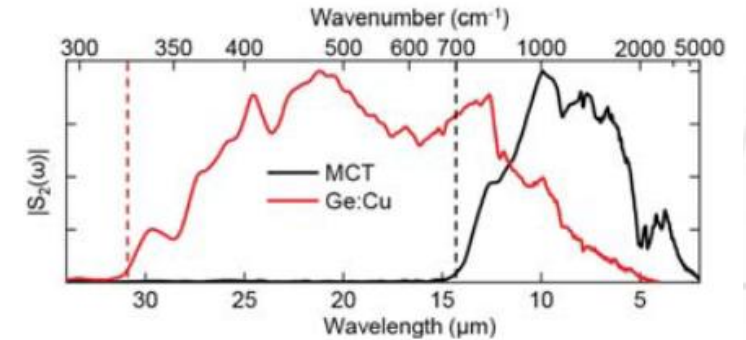
- FTIR spectrometer: measures samples 1-10 mm in size
 - Small samples are < 1mm
- Typical microspectroscopy samples:
 - < 1 mm
 - few μm to few cm
- The third dimension
 - Reflective samples: surface state ('skin depth' $1/\alpha$)
 - Transmission: thin samples, thickness: $\sim 0.1\text{-}30 \mu\text{m}$



- **Spatial dimensions**
 - X,Y,(Z)
 - Polarization: orientation sensitive
- **Spectral dimensions**
 - Coupling with UV and Visible observation
 - Near-IR (0.8-2.5 μm)
 - Mid-IR (2.5-25 μm or 2.5-50 μm (ISO 20473:2007))
 - Far-IR (25-250 μm)
- **Time dimensions**
 - Non-destructive
 - Evolution/aging
 - Phase transitions
 - Kinetics (μs – hours)

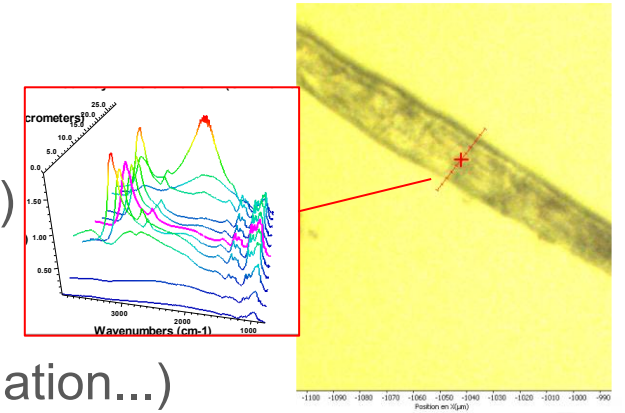


Liver cirrhosis tissue



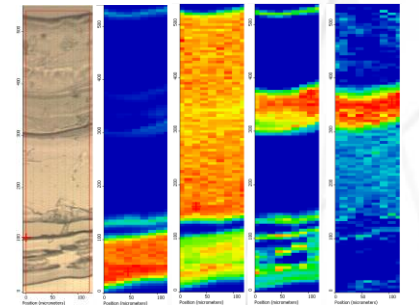
- **Small samples**

- Isolated individual particles (micro and nanoplastics, dust, grains...)
- Isolated fibres (polymers, hair, wool...)
- Single biological cells
- Material under constraints (temperature, pressure, stretching, irradiation...)
- Materials in extreme conditions (pressure, temperature...) Diamond Anvil Cells (DAC)
- ...



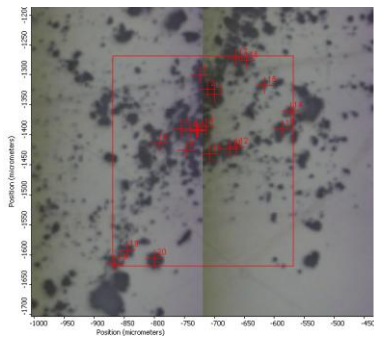
- **Mapping heterogeneous samples:**

- Individual particles **within** matrices (colorants in binder, grains in minerals, contaminants in polymers or on silicon wafers...)
- Multilayers (paintings, laminates ...)
- Interfaces, thin films
- Biological tissues
- Single cells

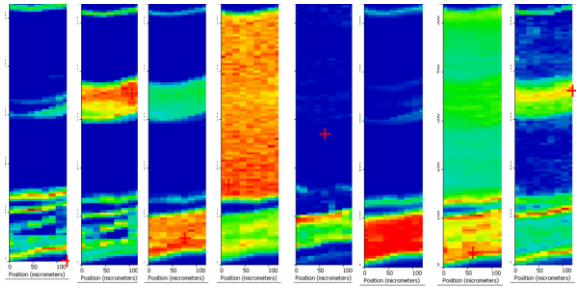


- ...

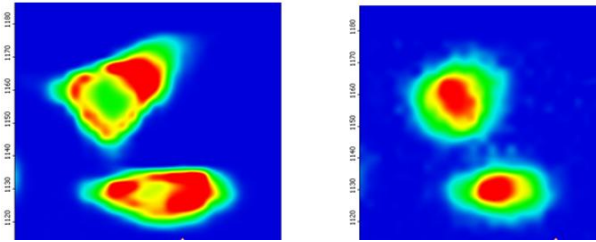
Particles



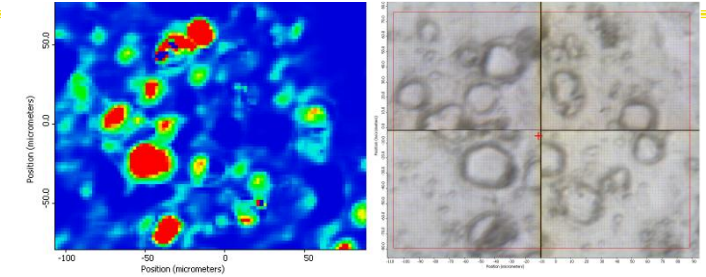
Polymer laminate



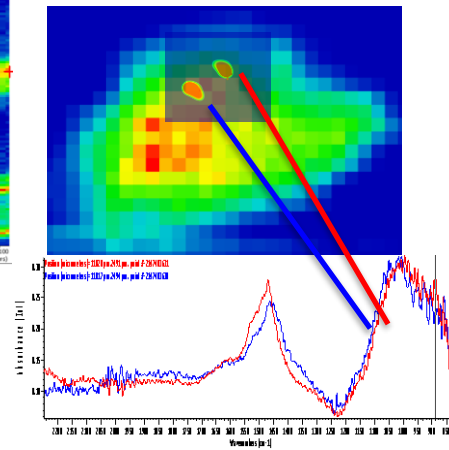
Single cells



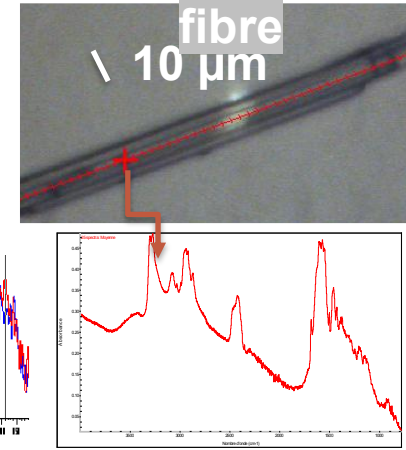
Inclusions



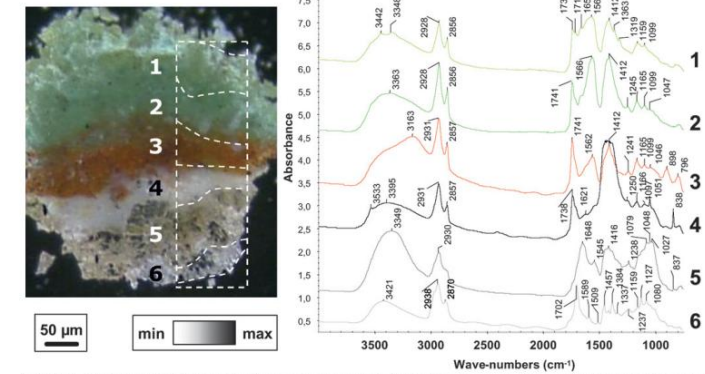
Asteroid grain



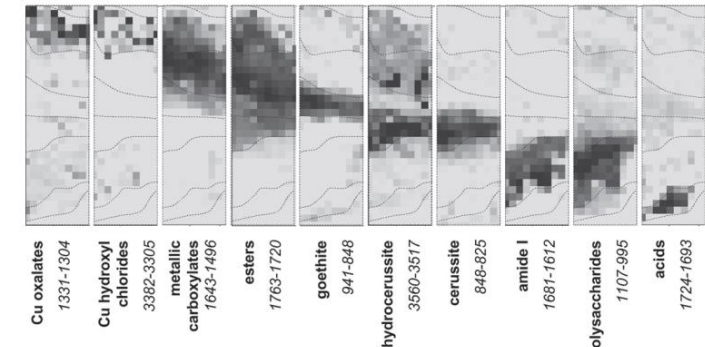
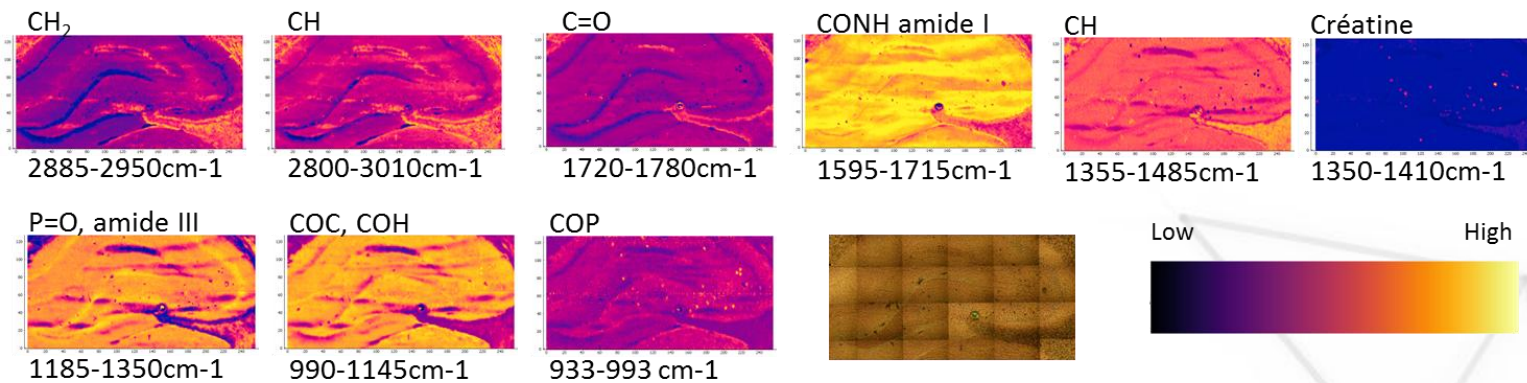
Protein fibre



Mural Paintings



Biological tissues



Cotte et al. J. Anal. At. Spectrom., 2008, 23, 820-828

- **PHYSICS**
 - MATERIAL IN EXTREME CONDITIONS
 - ELECTRONICS, BAND GAP, CHARGE CARRIER DENSITY
 - HIGH PRESSURES, HIGH TEMPERATURES
- **CHEMISTRY**
 - POLYMERS
 - CATALYSIS
 - SURFACES
 - ELECTROCHEMISTRY
- **BIOLOGY**
 - TISSUE SECTIONS
 - HARD TISSUES (bone, dentin, cartilage)
 - 2D/3D CELL CULTURES,
 - LIVING CELLS
 - BIOMATERIALS
 - DIAGNOSIS
 - COSMETICS (hair, skin, nails)
- **ENVIRONMENT**
 - PLANTS, PLANT CELL WALLS
 - SOILS
 - AEROSOLS
 - MINERALOGY & GEOLOGY
 - MICROPLASTICS
- **CULTURAL HERITAGE SCIENCES**
 - POLYCHROMY, PAINTINGS
 - RESINS, VARNISHES
 - MATERIALS woods, bones, ceramics...
- **ASTROCHEMISTRY**
 - METEORITES, MICROMETEORITES, **UCAMM** Ultra Carbonaceous Antarctic Micro-Meteorites
 - IDP Interplanetary Dust Particles
 - SPACE RETURN SAMPLES (Hayabusa 1/2, Stardust...)
- **FORENSICS**
- **PHARMACEUTICS**

Confocal Fourier Transform IR microscopy (μ FTIR)

- Conventional
- Synchrotron**

Hyperspectral FTIR Imaging

Direct Laser IR imaging

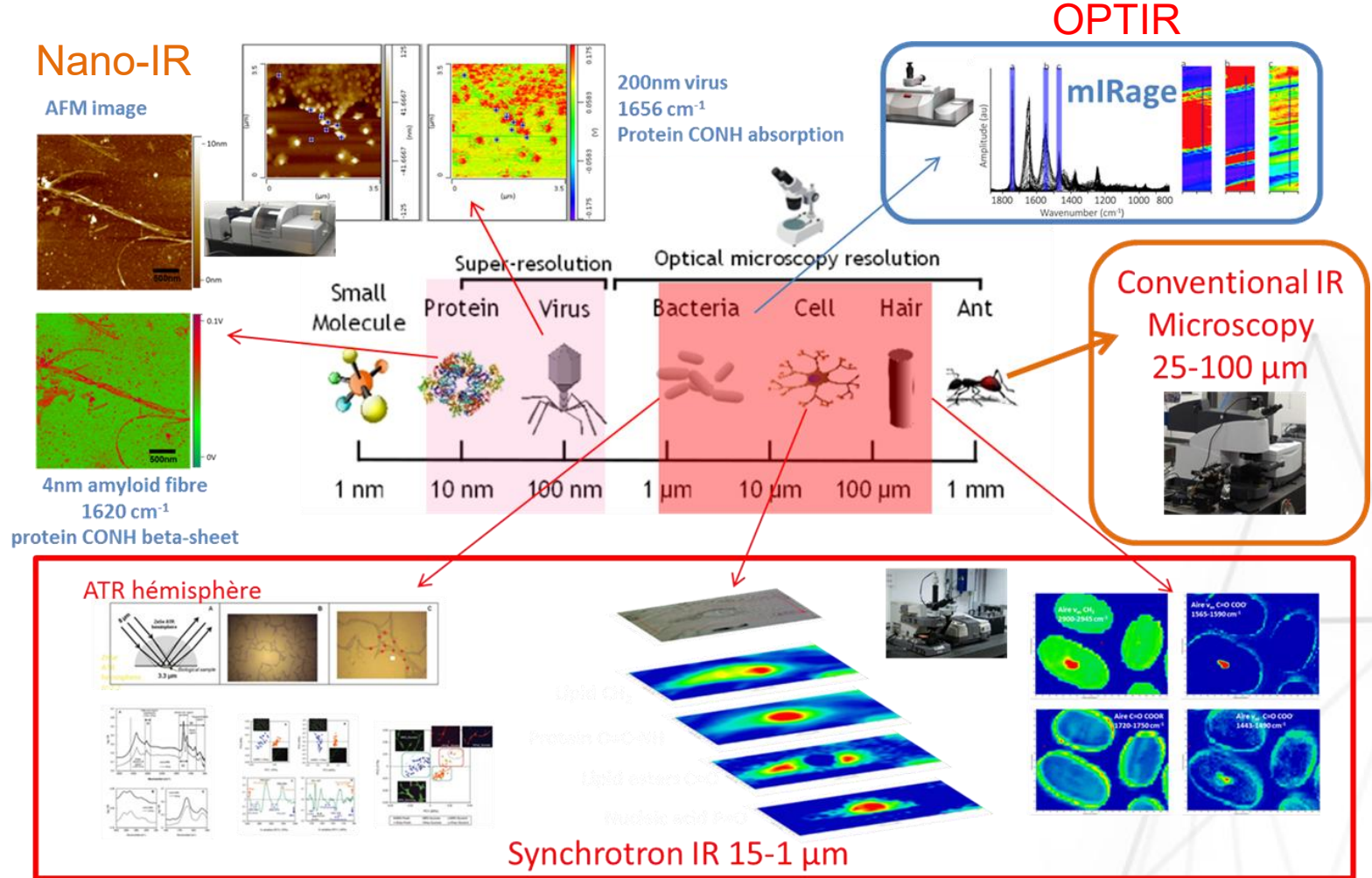
Optical Photothermal IR

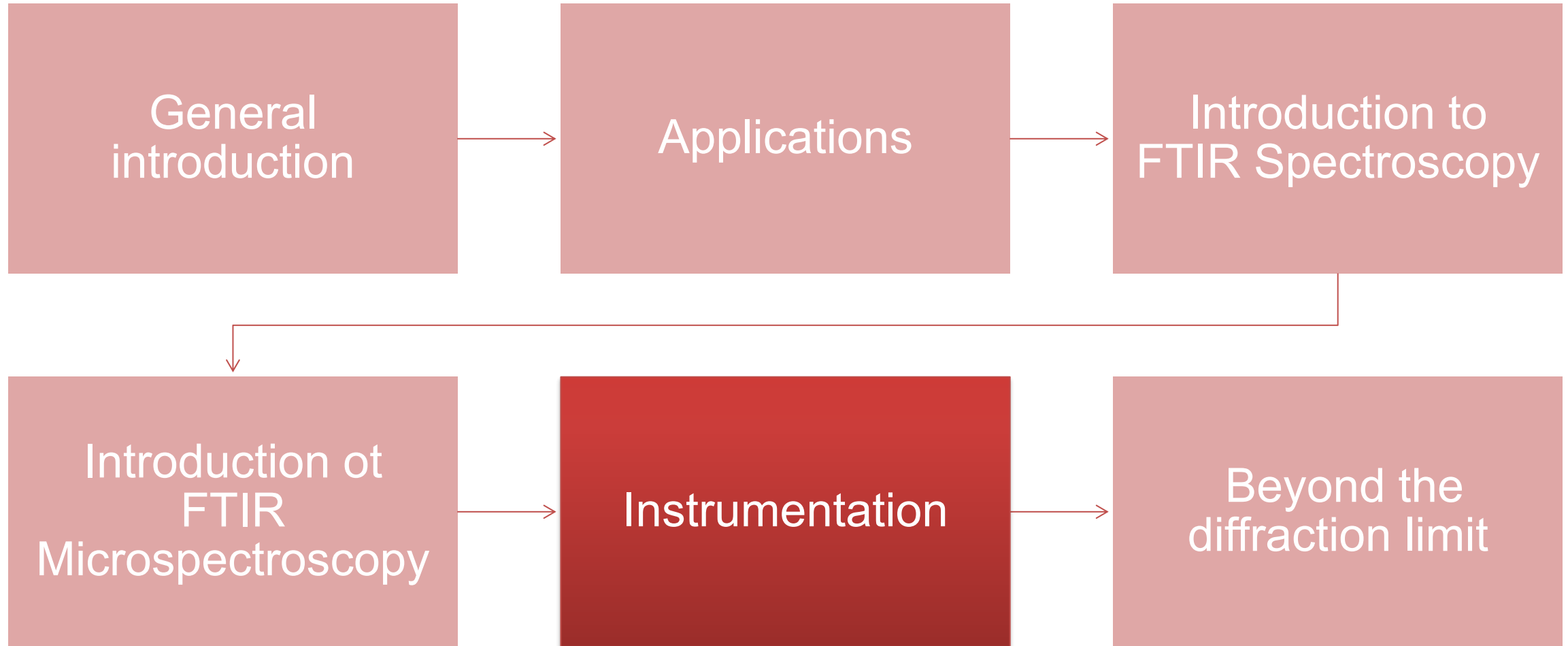
Nano-IR

- Photothermal (AFM-IR)
- Scattering (sSNOM)

Differ in:

- Measurement principle
- Spatial resolution
- Spectral range
- Samples and sample preparation
- Abilities (sensitivity, quantification, speed)





- Conventional source: globars

- SiC bar heated at 1200-1300K: black body radiation
- Stable, broadband (mid-IR)
- Cheap (500€)



- Synchrotrons

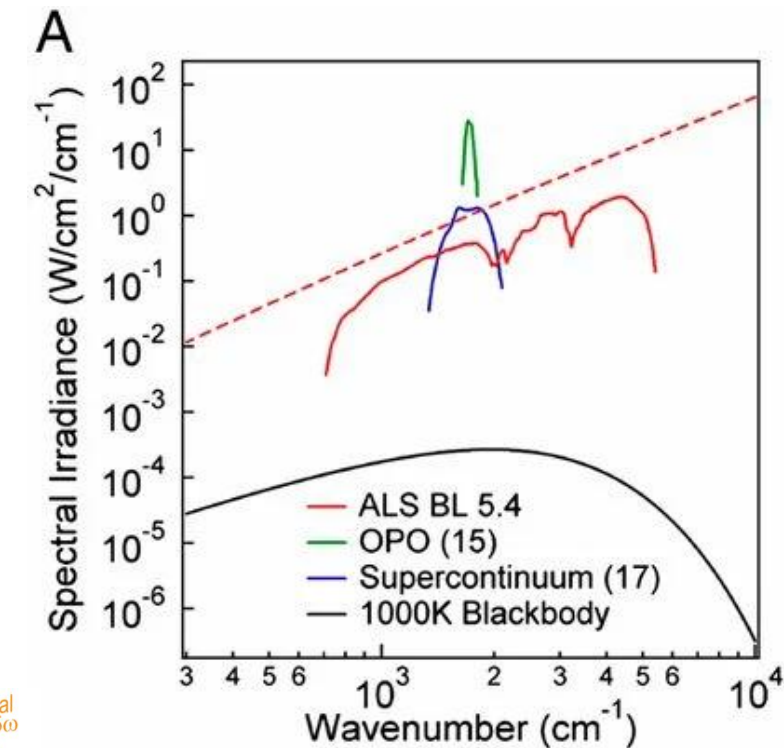
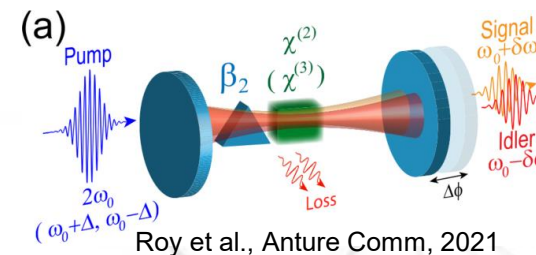
- Electrons accelerated at the speed of light
- **Ultrabroadband** (THz, far IR, mid IR, near IR ... hard X-rays)
- High brilliance
- Very expensive 500 M€, rare, **user facilities**



- IR lasers

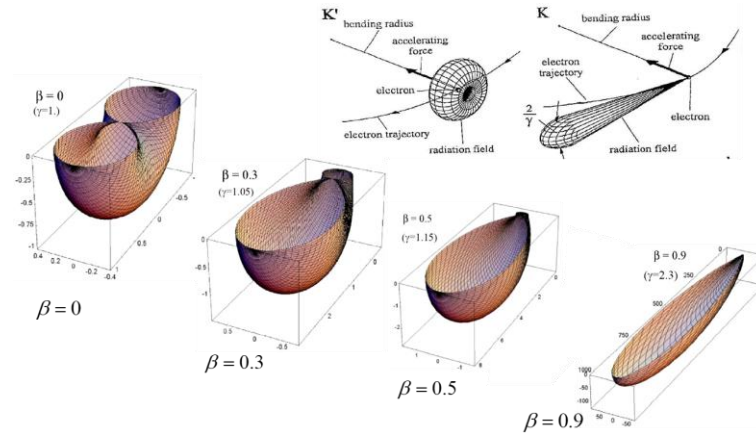
- Quantum Cascade Lasers (accordable)
- Supercontinuum lasers
- Optical Parametric Oscillators (OPO)

- Expansive (100 k€), rare
- Aggressive for sample
- Unstable

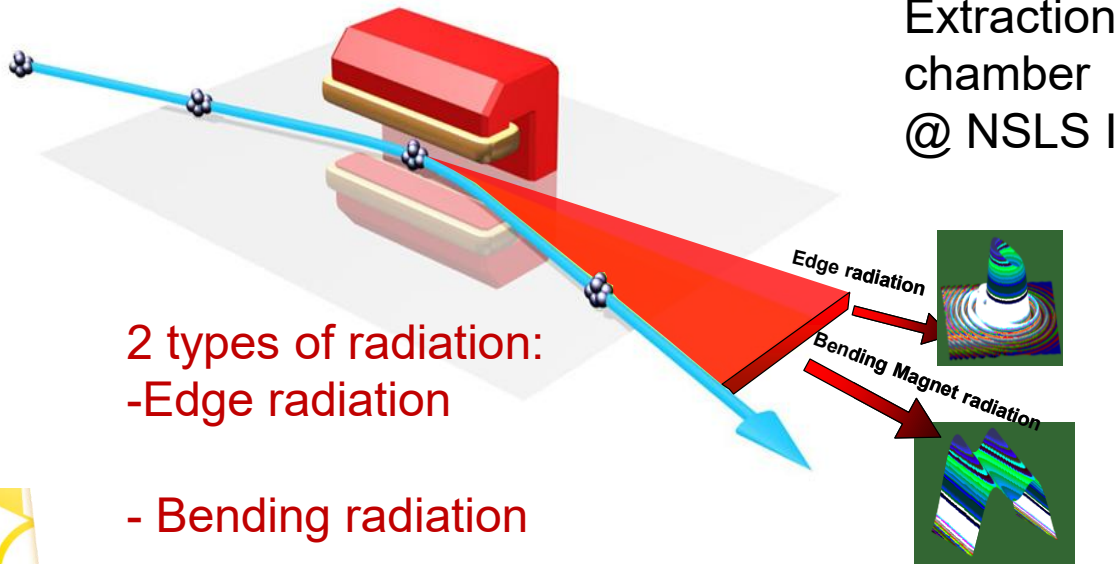


Bechtel PNAS 2014

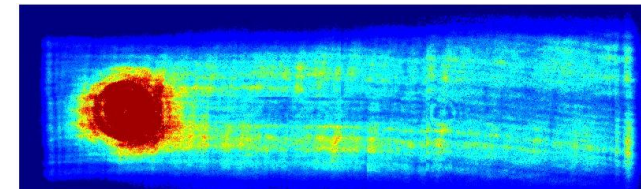
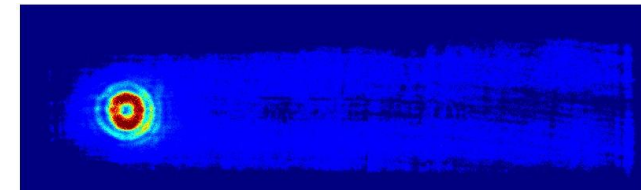




IR is generally collected with a slotted mirror from a **bending magnet source**:



Light map at $\lambda=500\text{nm}$



Polarization
 Edge radiation: circular
 Bending radiation: straight

2 types of radiation:
 -Edge radiation

- Bending radiation

IR flux is proportional to synchrotron current intensity

- COUPLING A SYNCHROTRON SOURCE TO AN IR MICROSCOPE

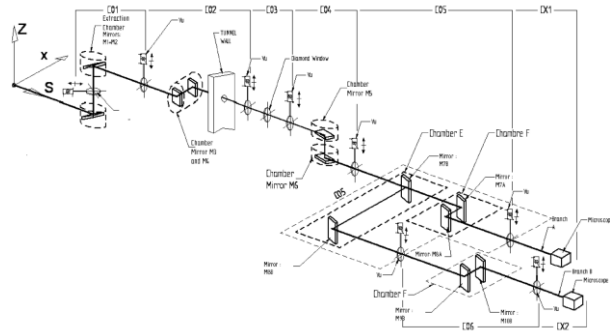
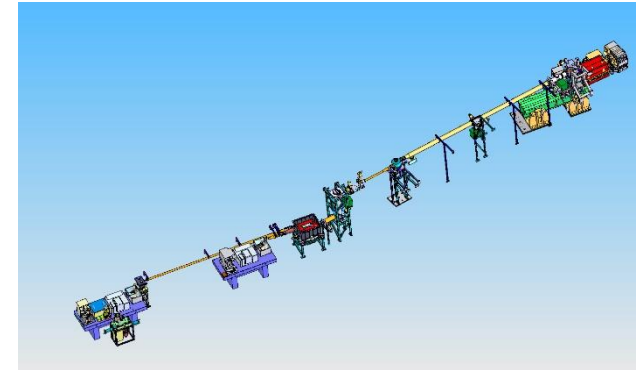
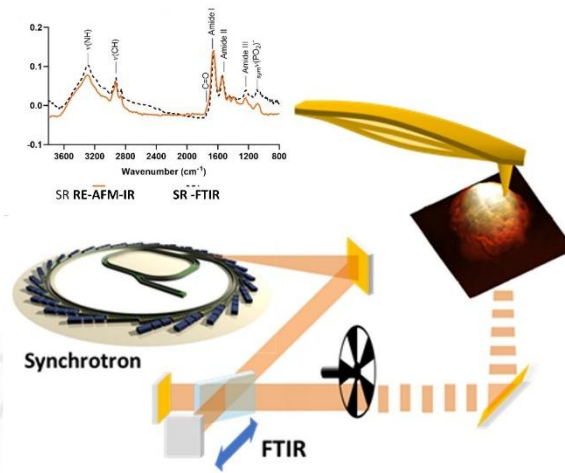
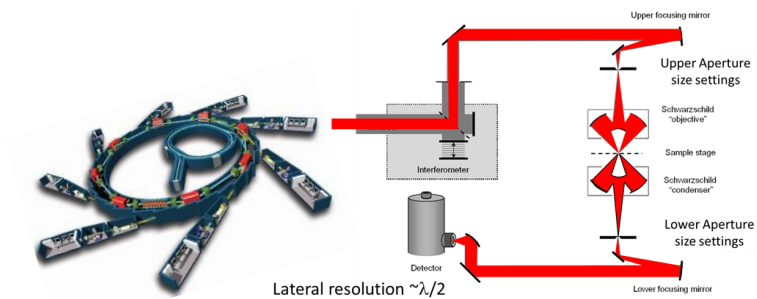


Fig. 7. The layout of the SMIS beamline at SOLEIL.



- CONFOCAL MICROSCOPY

NANO-IR

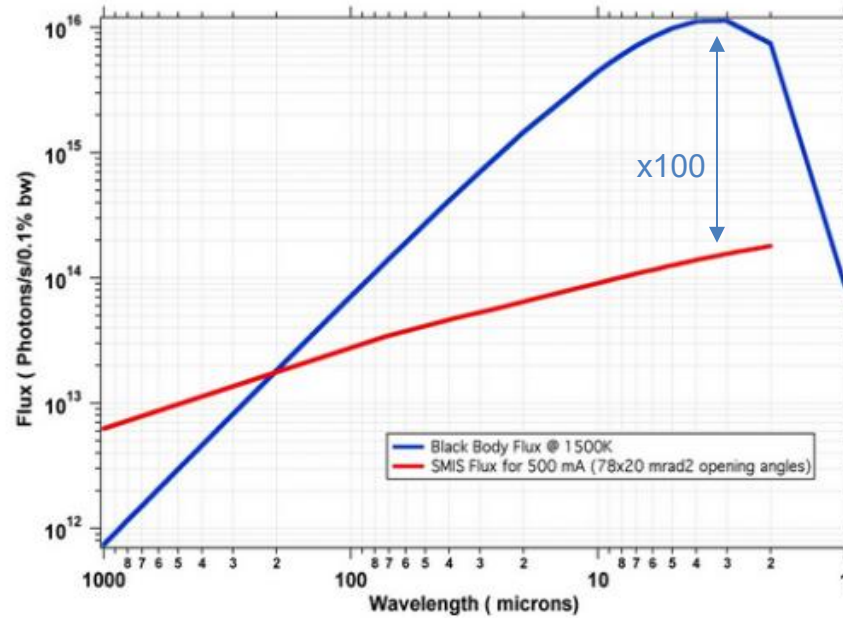


- Brilliance:

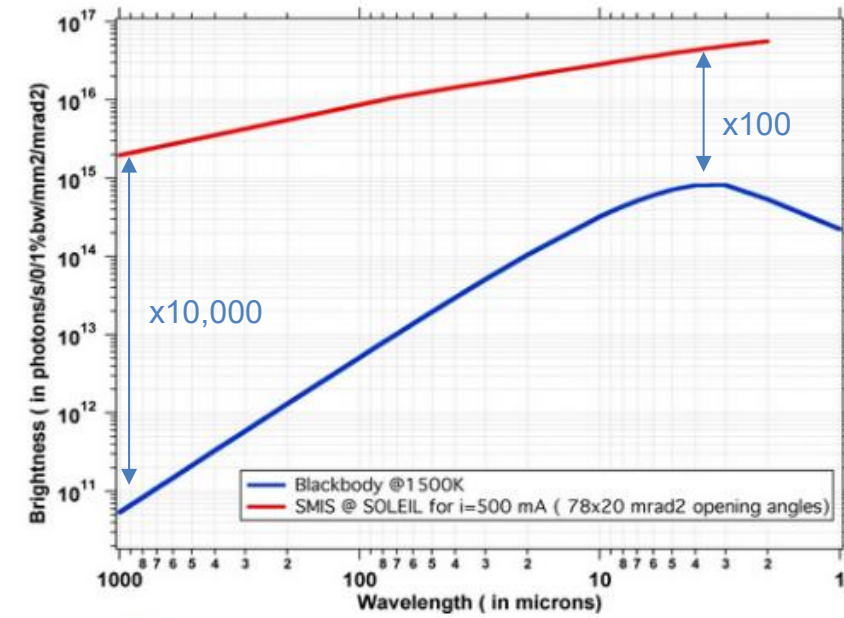
Black body thermal source (globar)
SOLEIL Synchrotron



FLUX



BRILLIANCE

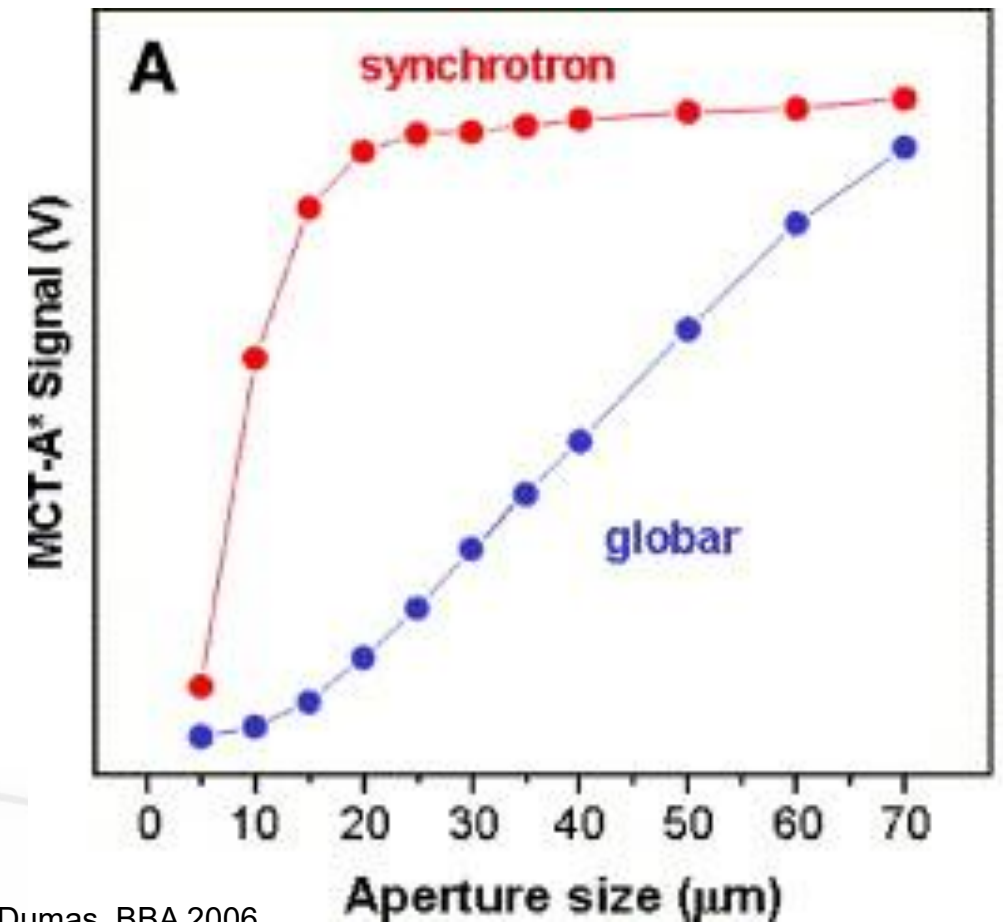
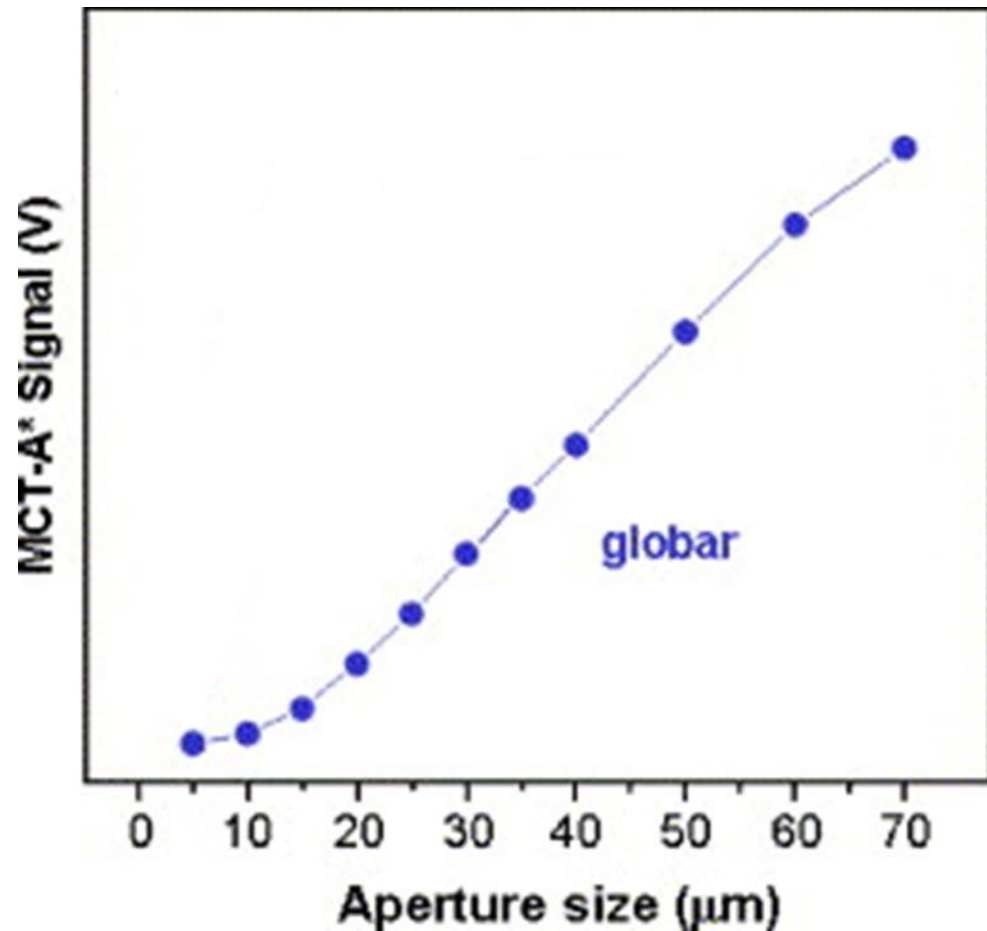


- Ultrabroadband:
 - From the THz
 - To the X-ray

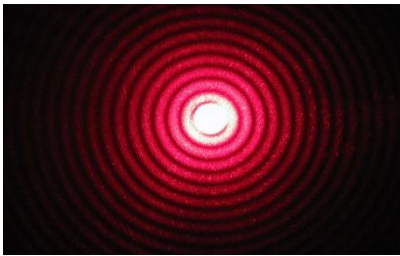


- Effect of the microscope aperture size on the IR signal

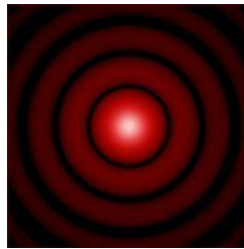
Signal versus confocal aperture size



- GENERATING A MICRO SPOT IN AN IR MICROSCOPE: **PINHOLES**



Diffraction pattern by a single pinhole

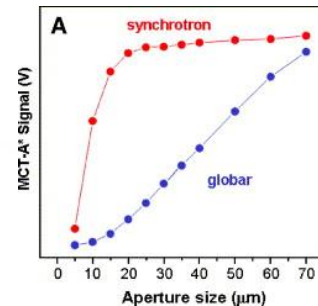
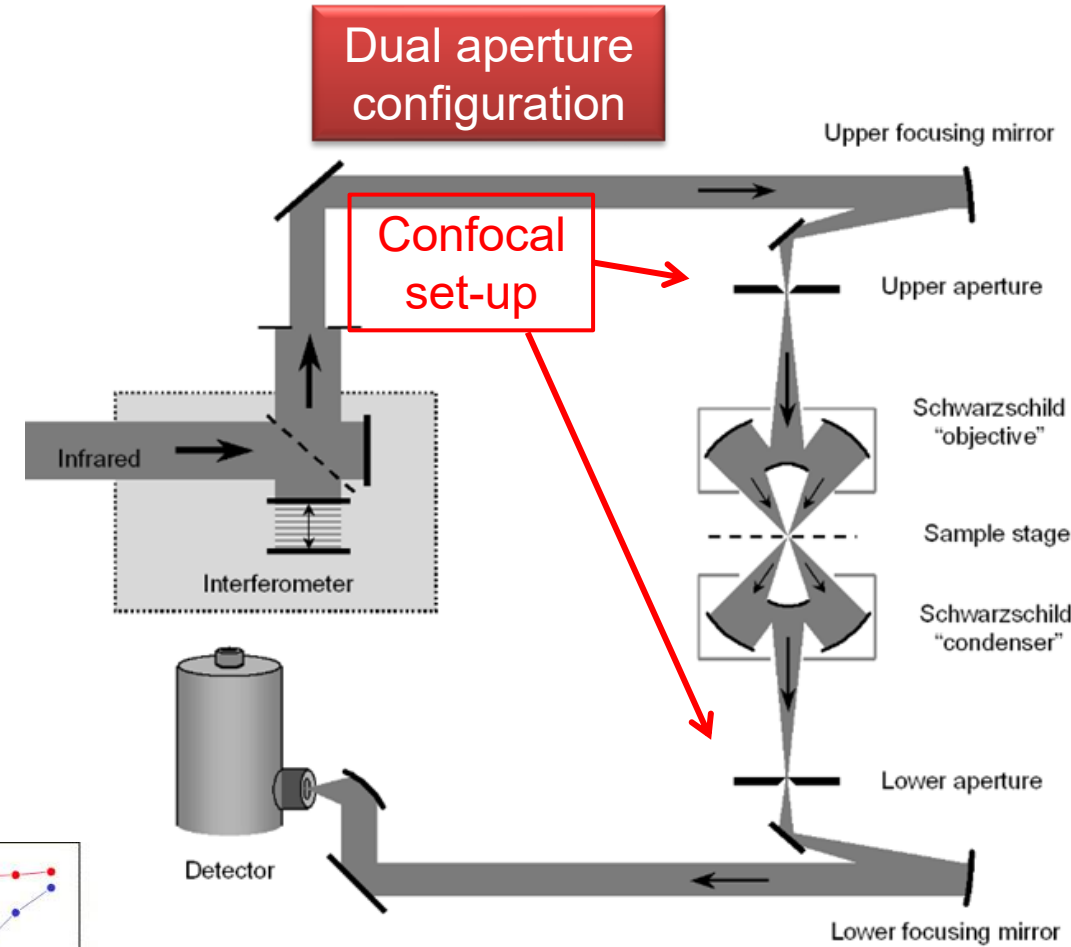


Diffraction pattern in a confocal system

Lateral resolution: $\sim \lambda/2$

Diffraction limits spatial resolution

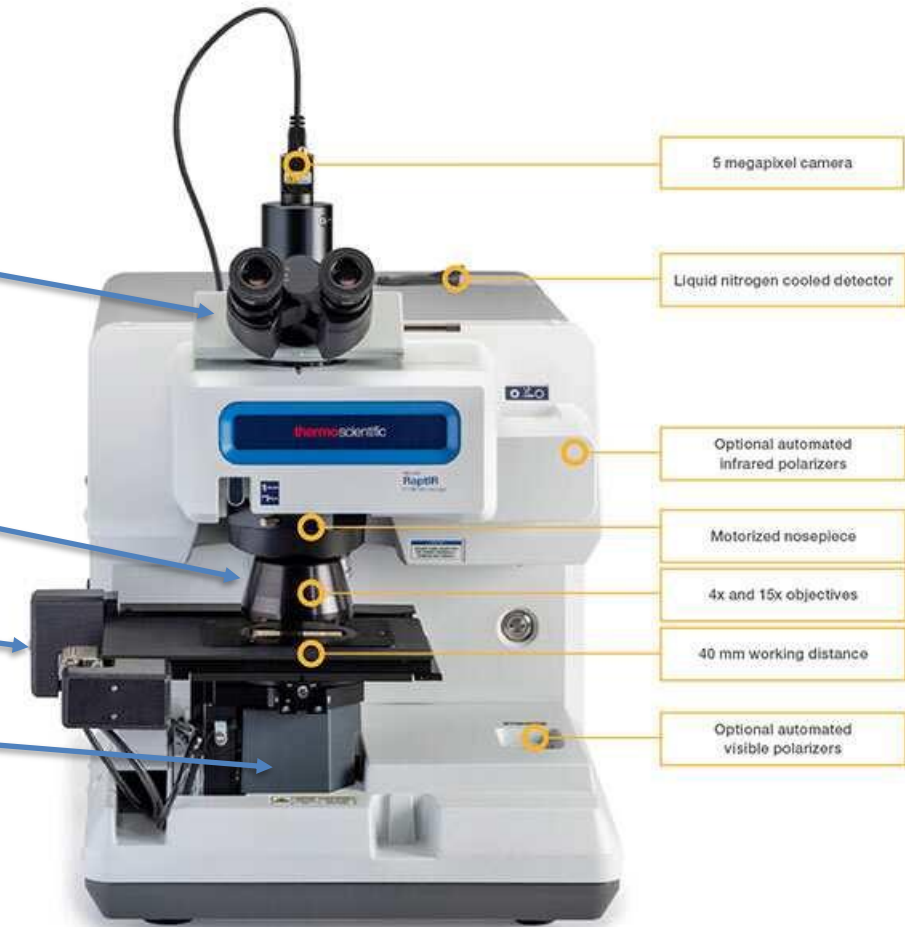
Confocal apertures reduce diffraction
Confocal apertures induce huge signal losses



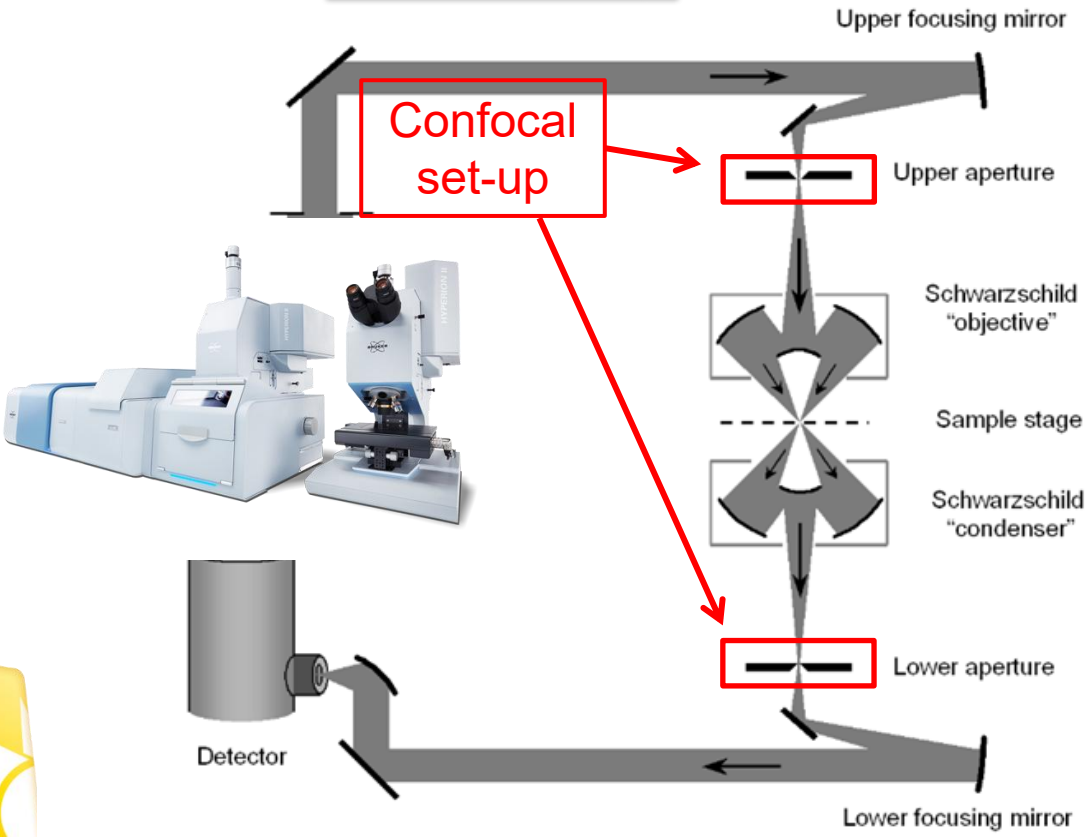
The **Confocal** FTIR microscope has been the staple of synchrotron IR beamlines for over 30 years



- Microscope mainframe
- Microscope optics
- Visualization (Binoculars, Camera)
- Illumination
- **Visible** and **IR** objectives
- IR detector(s)
- Motorized microscope stage
- **IR** Condenser
- Optional filters
- Beam ports



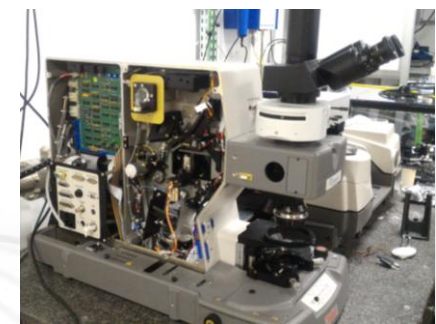
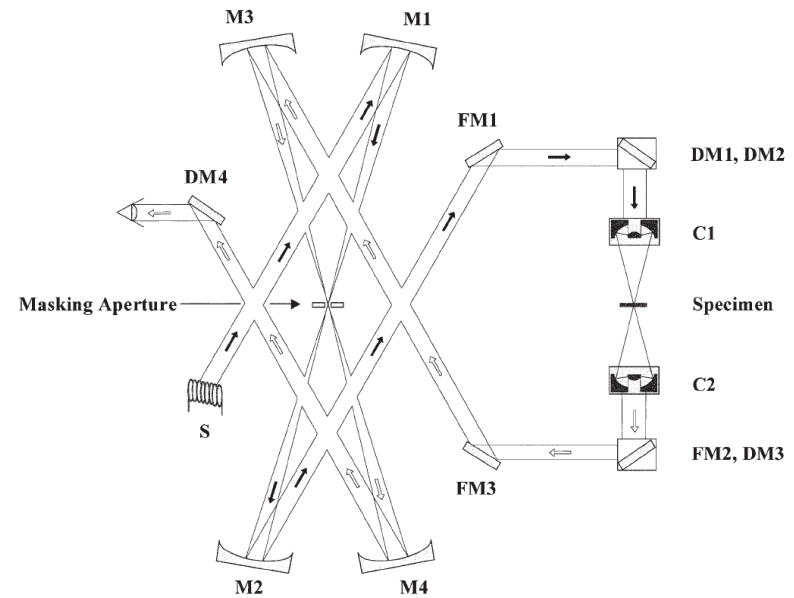
Dual aperture configuration



Single aperture configuration



Single aperture dual path configuration



ThermoFisher Scientific
Continuum

- Theoretical diffraction limit: given by Abbe equation:

$$R = \frac{0.61\lambda}{NA}$$

R: resolving power

λ : wavelength (μm)

NA: objective

Numerical Aperture,

NA= $n\sin(\theta)$

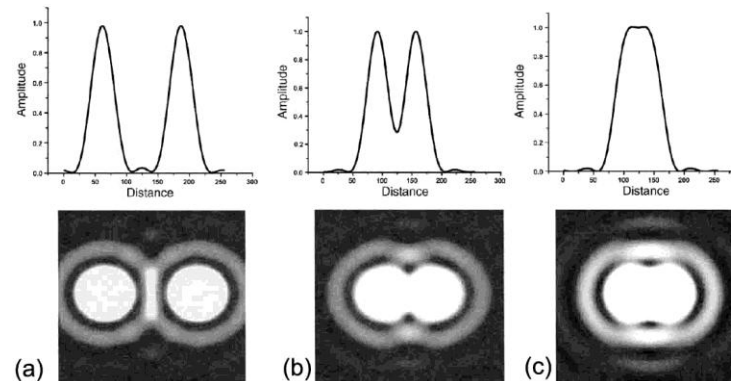
- Actual resolution will be worst due to:

- Diffraction from sample/optics
- Objective obscuration ratio
- Alignment
- In reflection mode

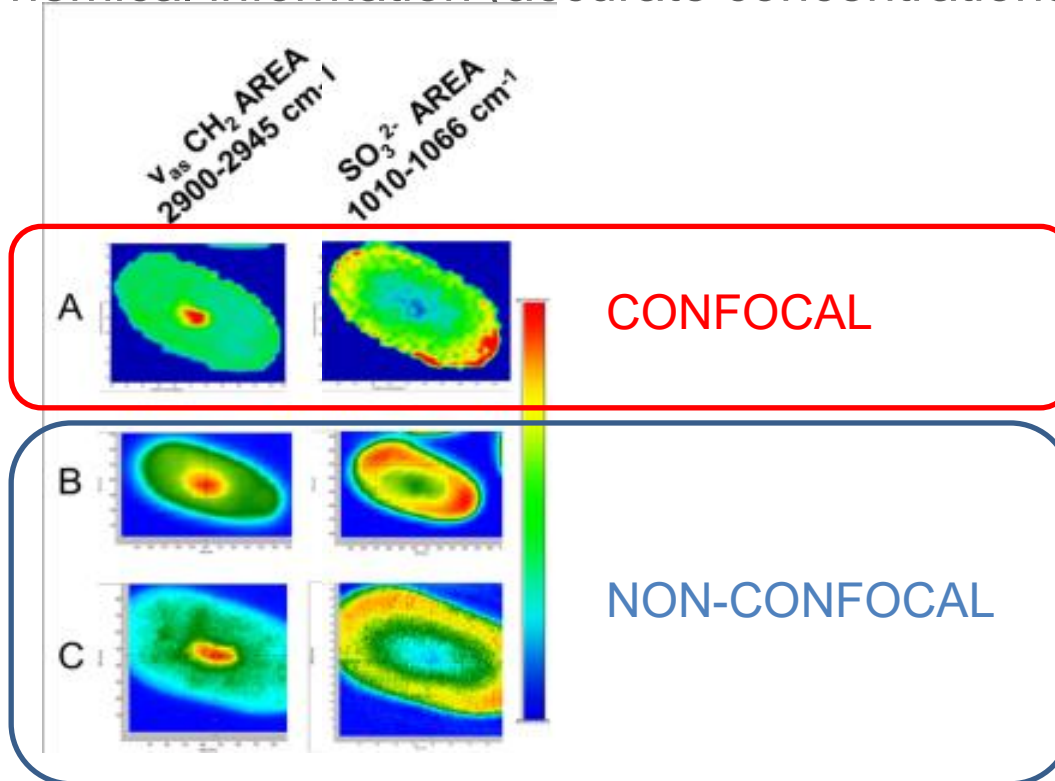
Typical NA for IR objectives:

15X objective: ~ 0.5

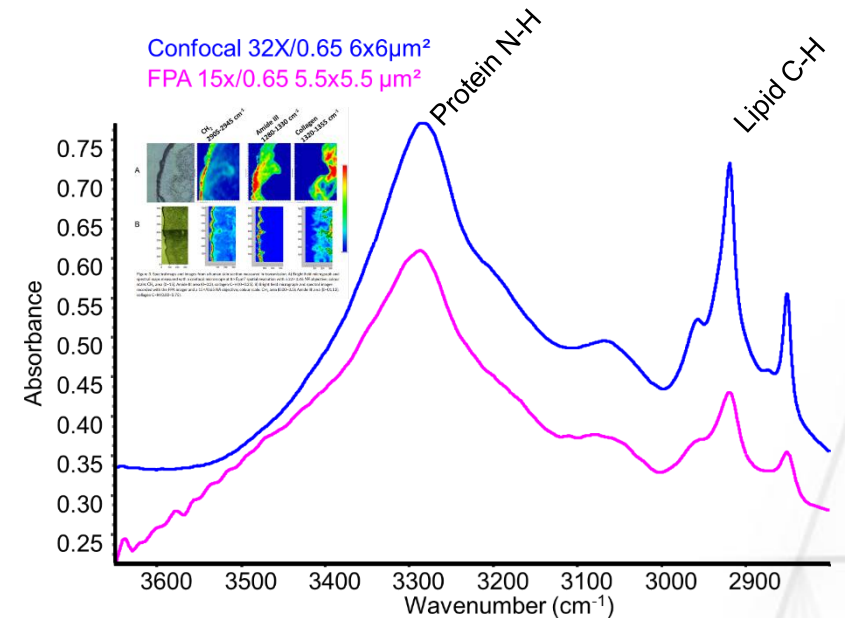
30X objective : ~ 0.6



- Spatial resolution is important for obtaining accurate information
 - Spatial information (accurate images)
 - Chemical information (accurate concentrations)



- Spectral images and maps of the same hair medulla
- Confocal microscope with synchrotron source
 - Low magnification imaging system (15x)
 - High magnification imaging system (62x)

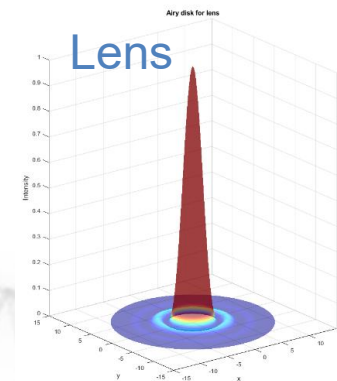
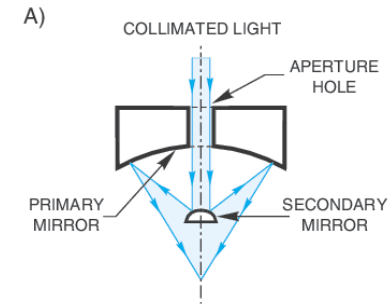


Spectra of the medulla of the same skin stratum corneum layer measured with either:

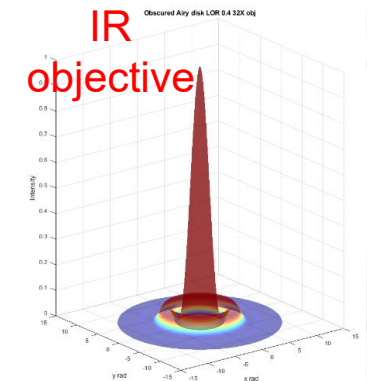
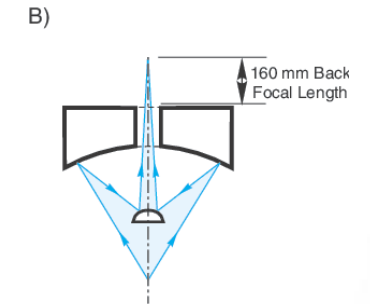
- A confocal microscope with synchrotron source at $6 \times 6 \mu\text{m}^2$ resolution
- A non-confocal IR microscope with FPA detector at $5 \times 5 \mu\text{m}^2$ projected pixel size

- IR objectives
 - All reflective spherical objectives
 - Avoid chromatic aberrations over the whole spectral range
 - Schwarzschild: focus to infinity
 - Cassegrain: focus to a focal point
- Central obscuration
 - Reduced throughput
 - Reduced resolution
 - Lower energy in the central lobe
 - Higher energy in the lateral lobes
- Objective magnifications
 - 15X
 - 25X, 30X, 32X, 36X, 40X
 - N.A. 0.5 - 0.8

Schwarzschild

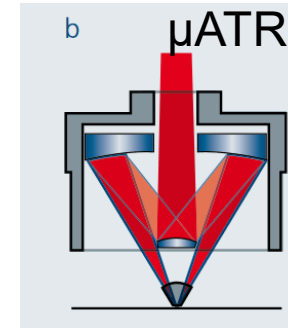


Cassegrain

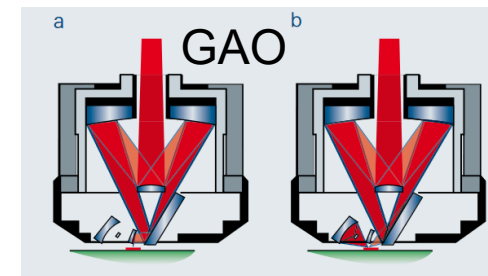


- **Attenuated Total Reflection (μ ATR)**
 - Used for thick, non-reflective samples
 - Contact sample: potentially destructive
 - Diamond, ZnSe, Ge
 - **Improved spatial resolution:** refractive index
 - Diamond 2.4
 - ZnSe 2.2
 - **Ge: 4**

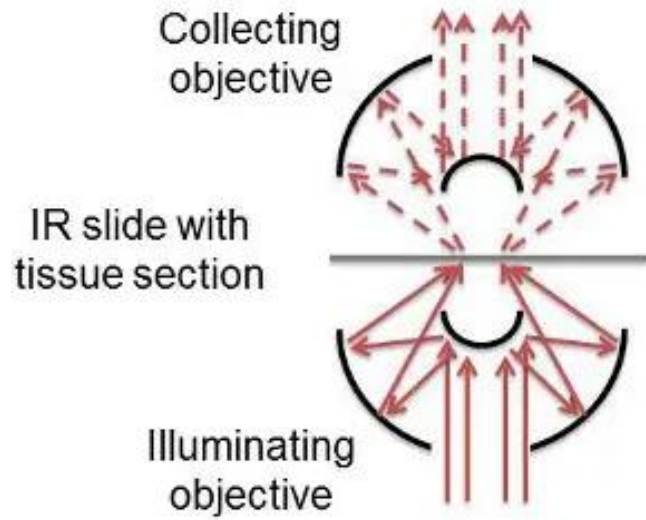
- **Grazing incidence objective (GAO)**
 - Improved sensitivity for oriented materials



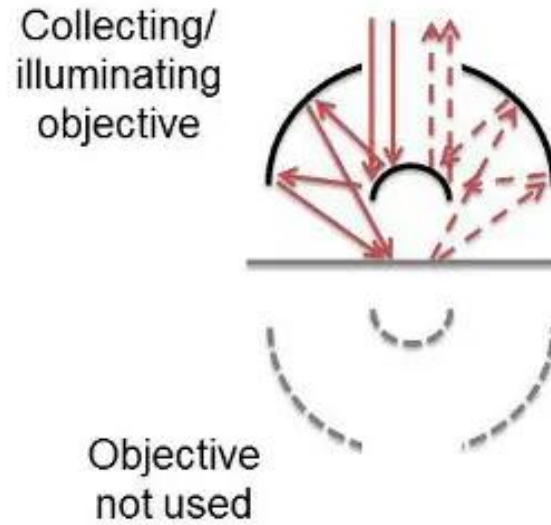
Artisan Technology Group



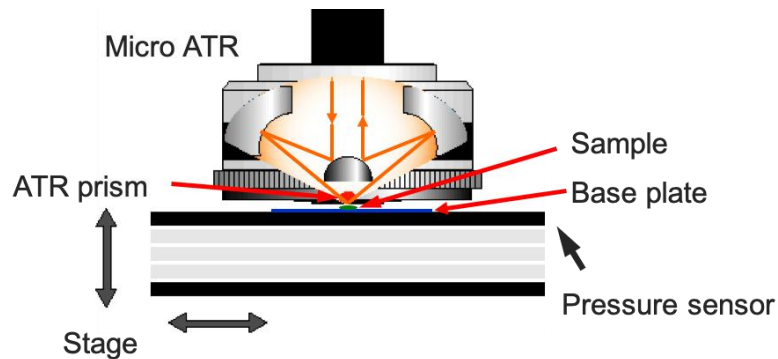
A) Transmission-mode



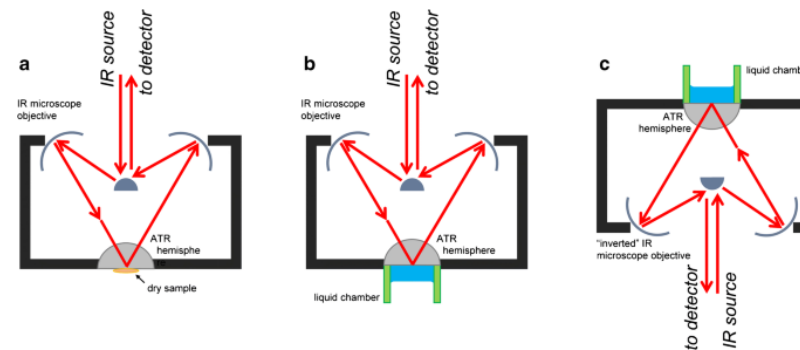
B) Reflection-mode



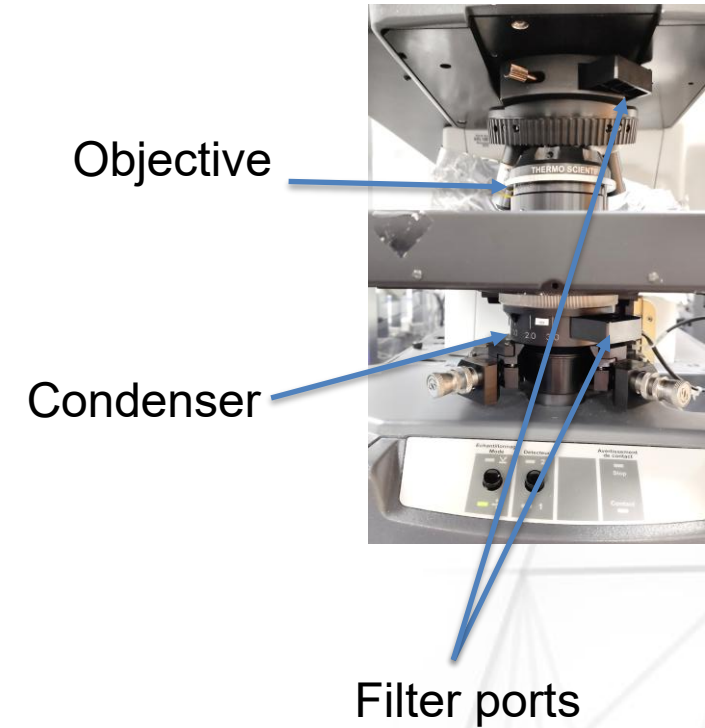
C) micro ATR mode



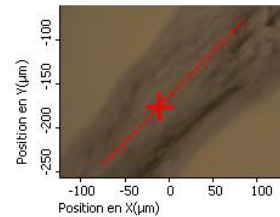
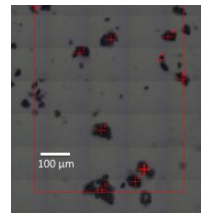
D) Inversed micro ATR mode



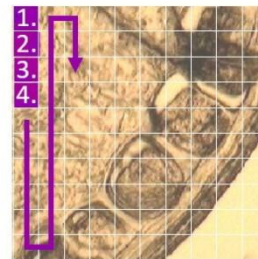
Transmission mode



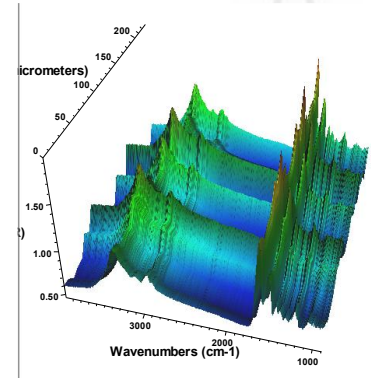
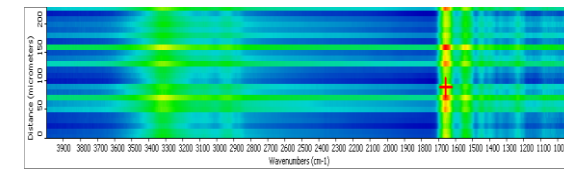
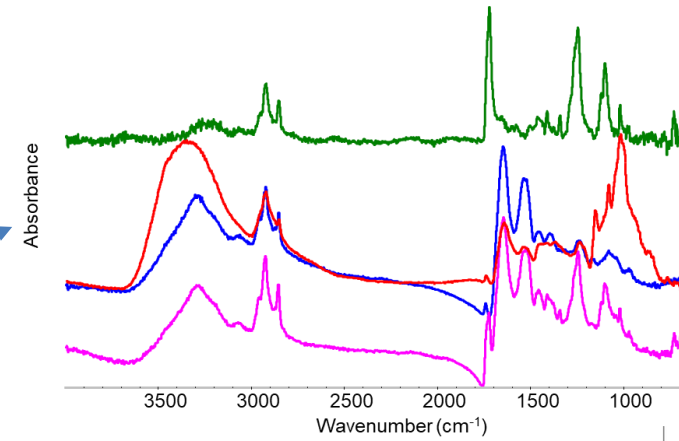
- Computer controlled motorized stage
 - 1 μm precision (0.1 μm optional)
- Discrete maps
 - Point by point
- Line maps
 - Across interfaces
- Area maps
 - Raster scanning
 - Sequential: slow



Single Element

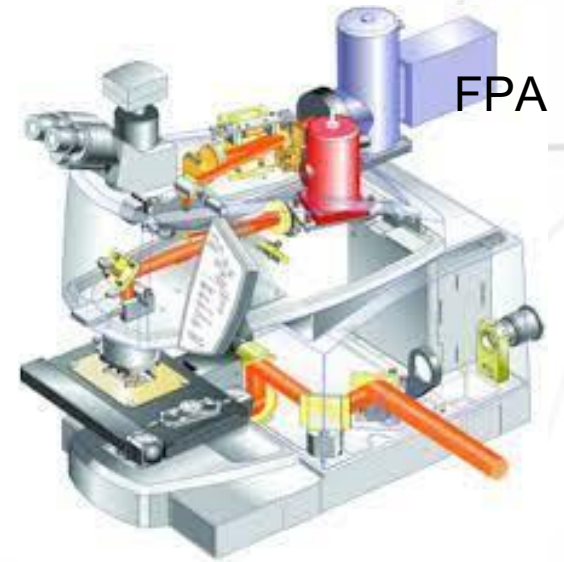
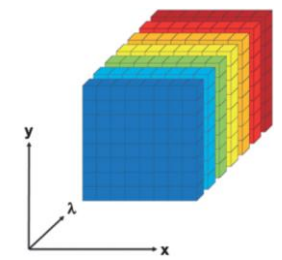
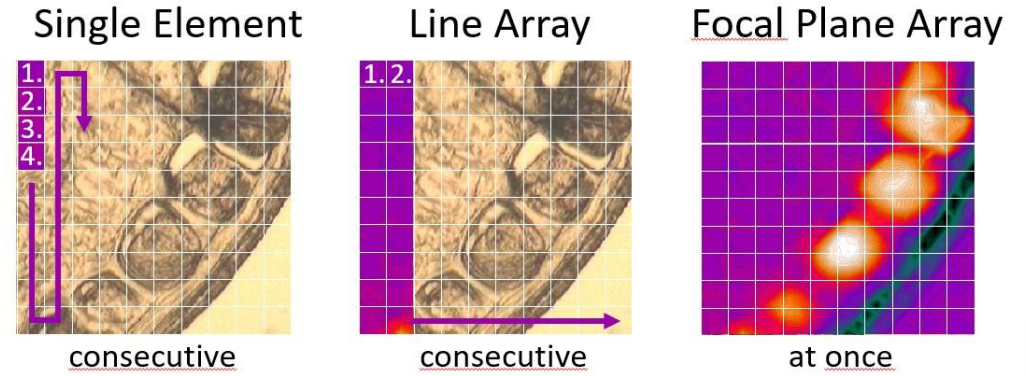


consecutive

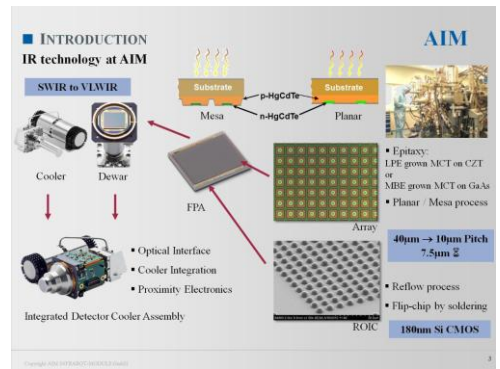


Time consuming

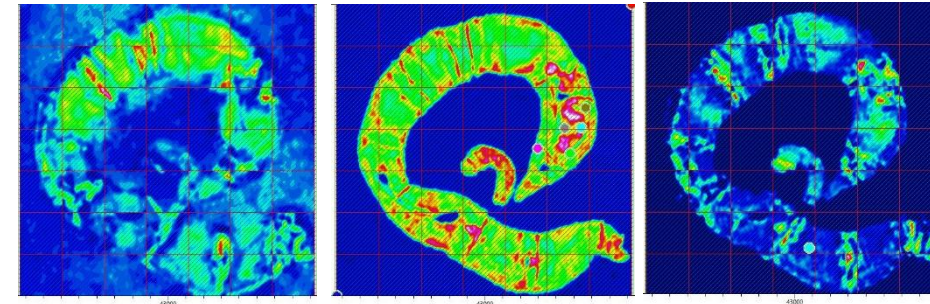
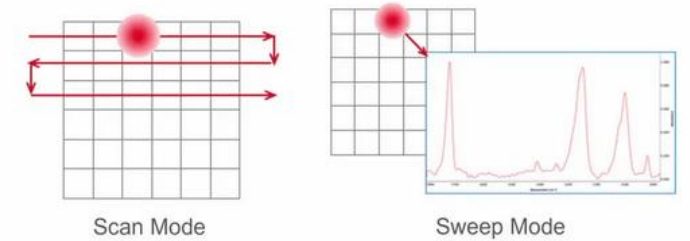
- Array detectors
 - Linear arrays
 - Focal Plane Arrays (FPA)
 - Use global source
- Each pixel contains a full spectrum
 - Hyperspectral image/hypercube of data
- Detector technology: narrow-band MCT



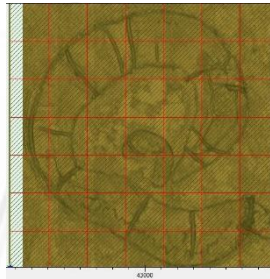
Agilent Cary 620 + Lancer FPA



- LDIR: LASER DIRECT IMAGING
- Couple QCL source and point MCT or FPA detector
- Can operate in two modes:
 - Imaging/scan mode: single wavelength
 - Spectral/sweep mode: acquisition of a full spectrum
- Transmission or reflection modes



S. mansonii worm

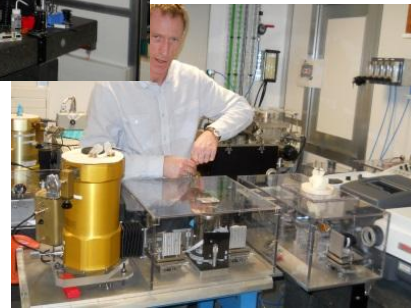
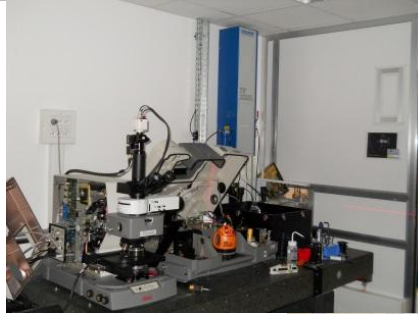
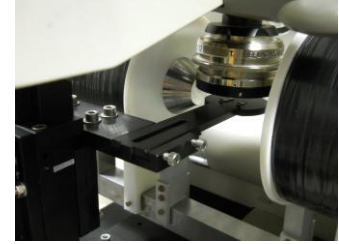
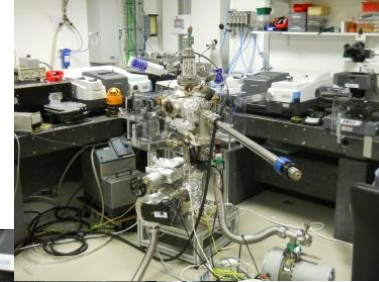


Agilent 8700 LDIR Chemical Imaging System



Bruker Hyperion II ILIM

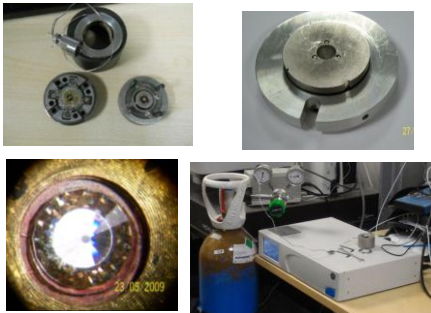
Endless possibilities



Physico-chemical constraints

Compression

Diamond Anvil Cells

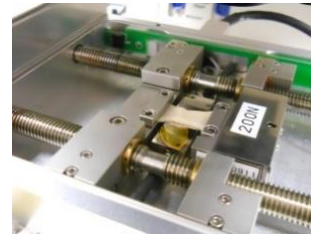


$10^1 - 10^6$ bars

Diamond compression cells
For flattening samples



Stretching



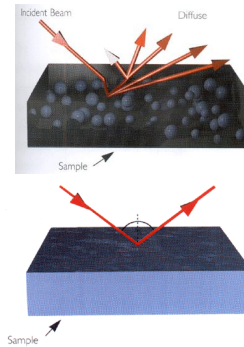
Heating/cooling atmospheric control



Fluorescence Imaging



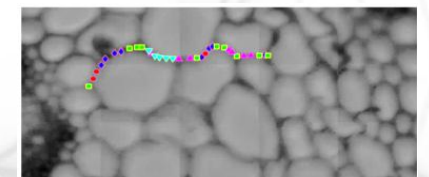
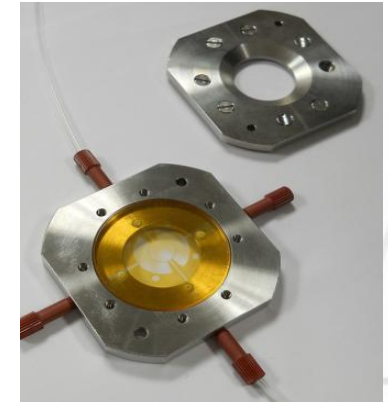
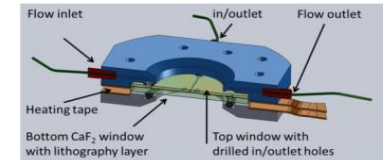
Réflexion

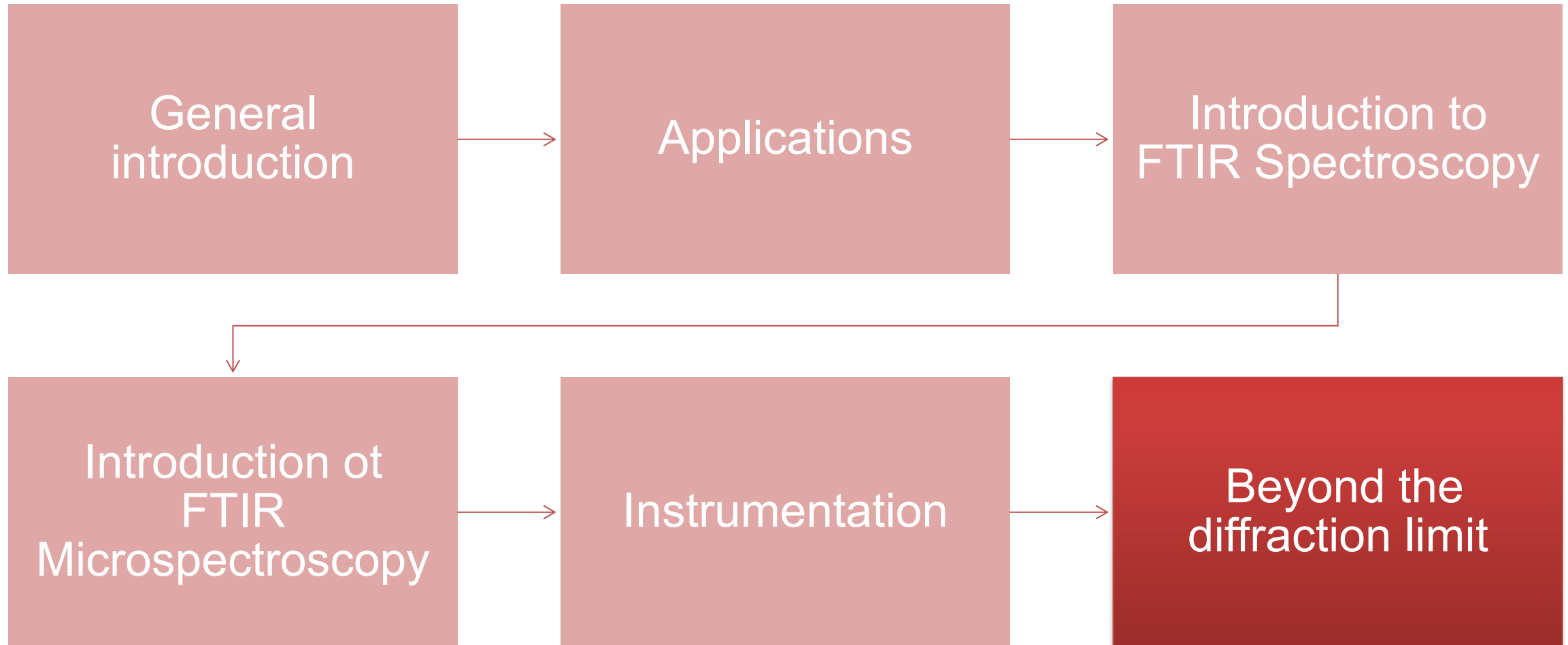


Micro-ATR
Inverted ATR

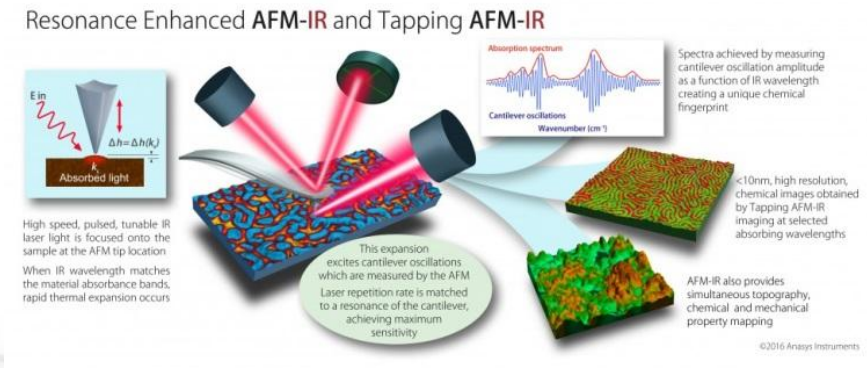
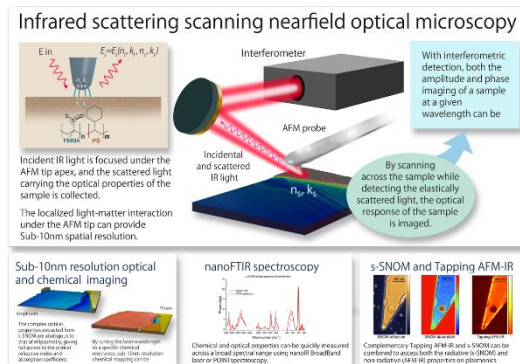
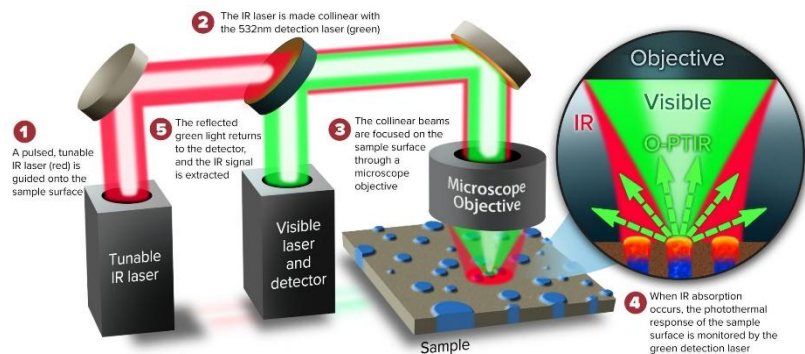


Microfluidics

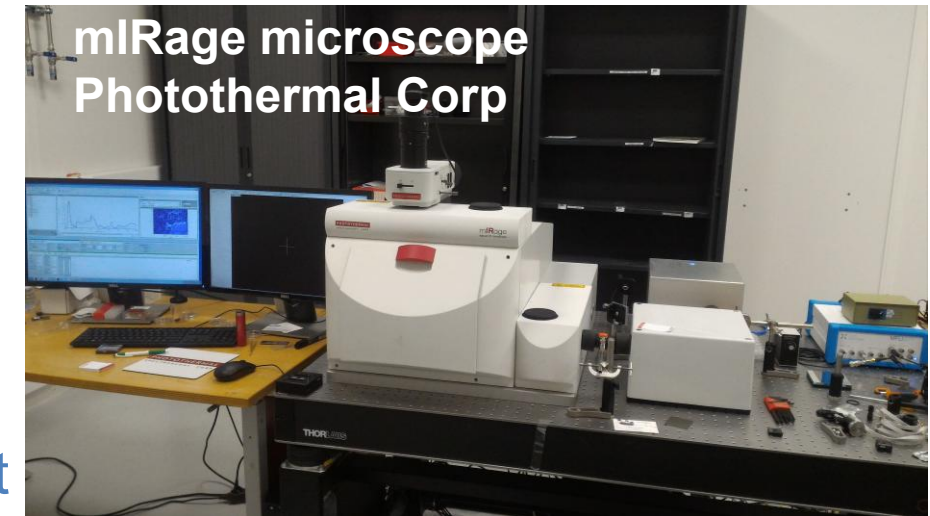
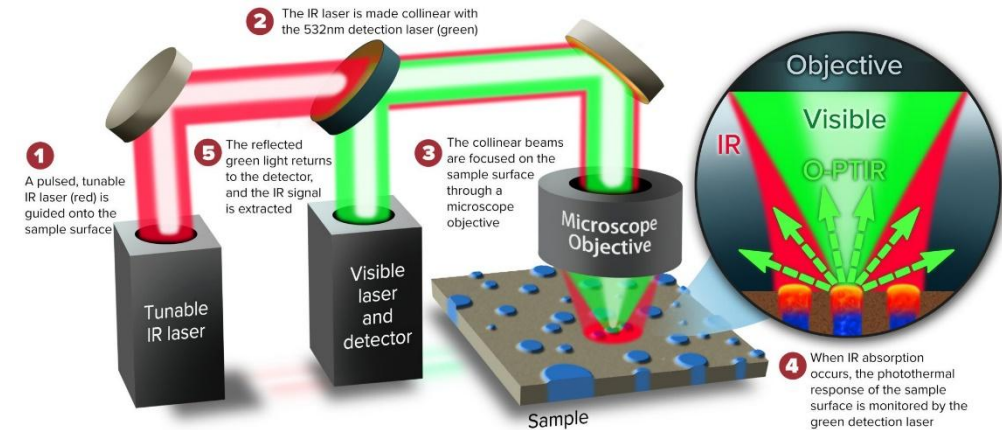




- Spatial resolution of IR microspectroscopy inherently limited by diffraction
 - 2.5-25 μm in the mid-IR
- Most of modern microscopy is done below the diffraction limit of IR:
 - Confocal laser fluorescence microspectroscopy
 - Nano particles (< 100 nm)
- New methods:
 - Optical PhotoThermal IR (OPTIR) : 250-500 nm resolution
 - NanoIR: 10-50 nm resolution



- Pump probe technique
 - QCL pump
 - Visible laser probe
- Measures change in sample refractive index n (“Mirage” effect)
 - n changes by a few % upon IR excitation
 - Triggers change in sample reflectivity
 - Green light can be monitored by very sensitive visible detectors (CCD, PMT, APD...)
- Spatial resolution given by the green laser
 - Diffraction limited in the visible
 - Co-propagation/counter-propagation the lasers
- Hardly compatible with synchrotron at the moment



Article

Broadband Fourier-Transform Optical Photothermal Infrared Spectroscopy and Imaging

Aleksandr Razumtcev, Gwendylan A. Turner, Sergey Zayats, Ferenc Borondics, Aris Polyzos, Garth J. Simpson*, and Hans A. Bechtel*

Analytical Chemistry 2025, 97, 37, 20117-20126 (Article) [Open Access](#)

Publication Date (Web): September 11, 2025

DOI: 10.1021/acs.analchem.5c02493

[Abstract](#) [Full text](#) [PDF](#)

ABSTRACT

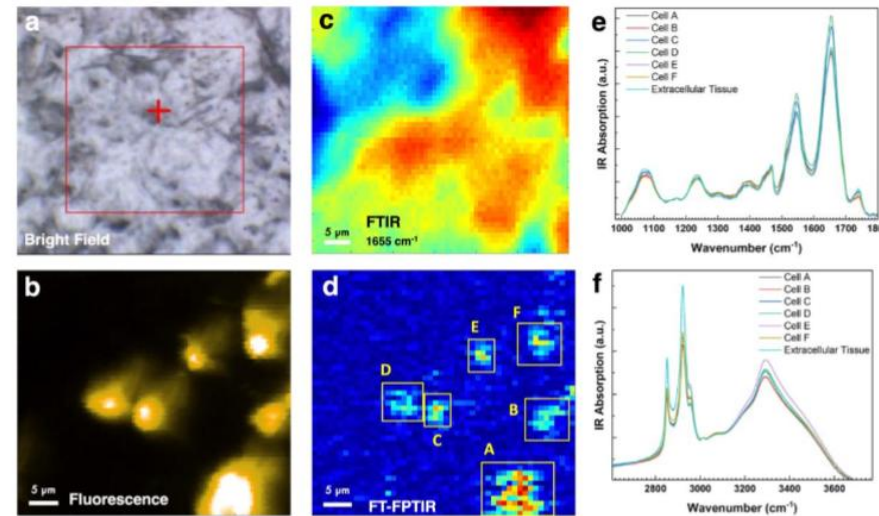
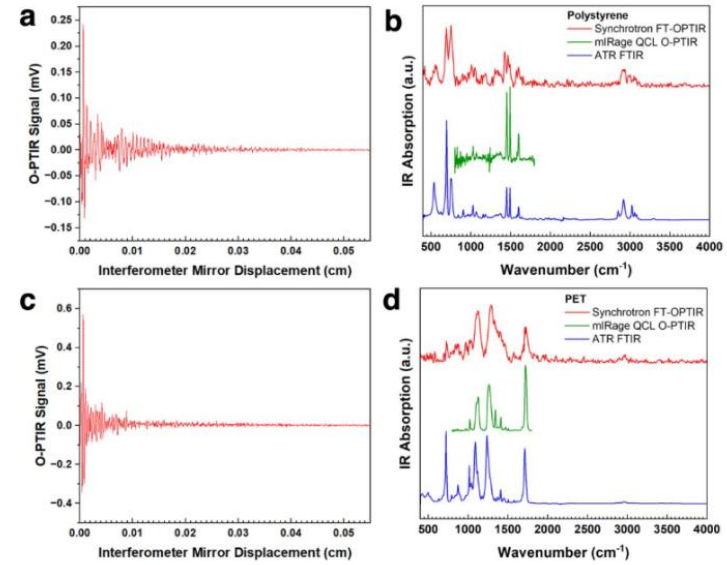
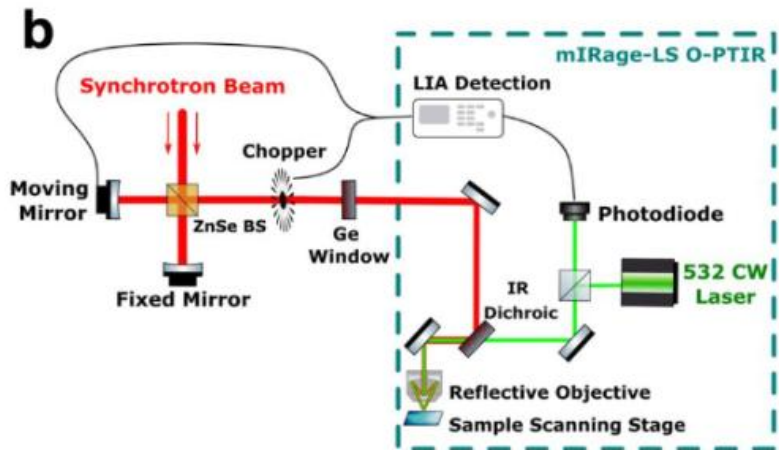
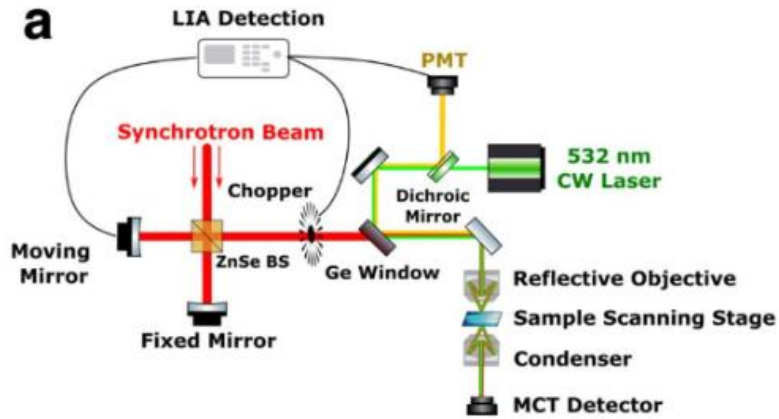
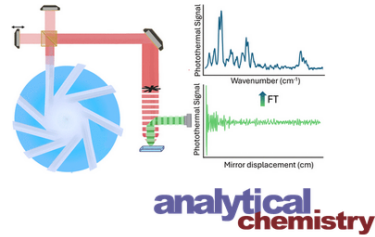
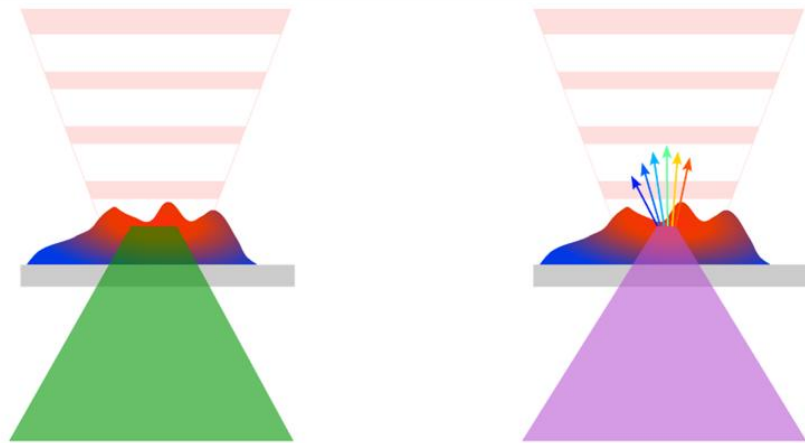
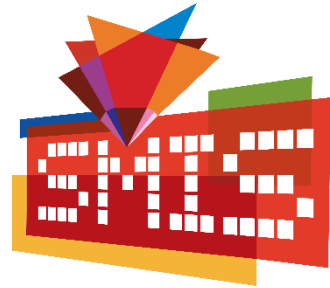


Figure 4. Cell-specific broadband FT-FPTIR chemical imaging of a fluorescently-labeled mouse tissue

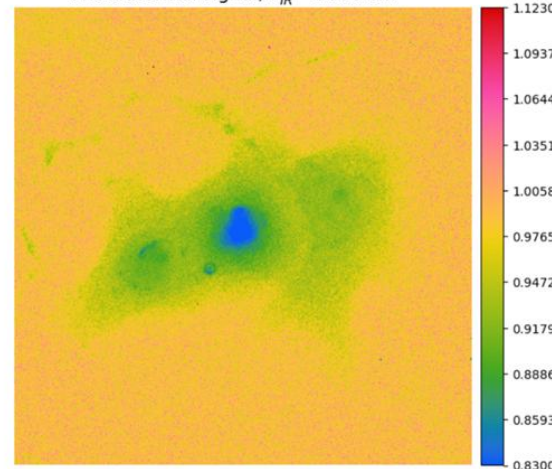
Synchrotron Radiation – UV – FL uorescence OPTIR

HIGHER RESOLUTION OPTIR



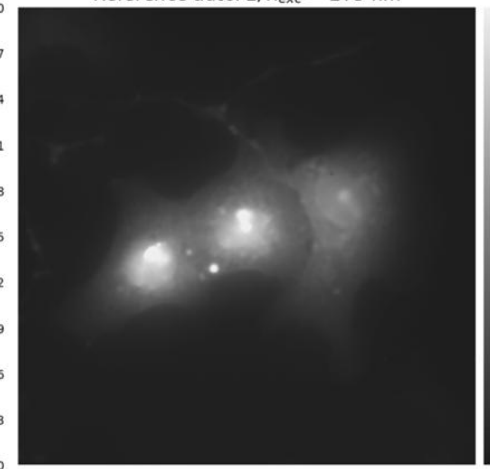
First SR-UV-FL-OPTIR images

Photothermal signal, $\nu_{IR}^* = 1660 \text{ cm}^{-1}$

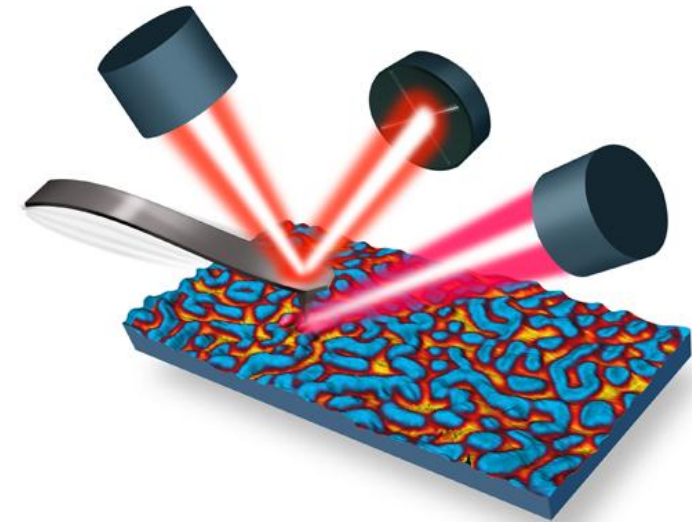


140 nm pixel size!

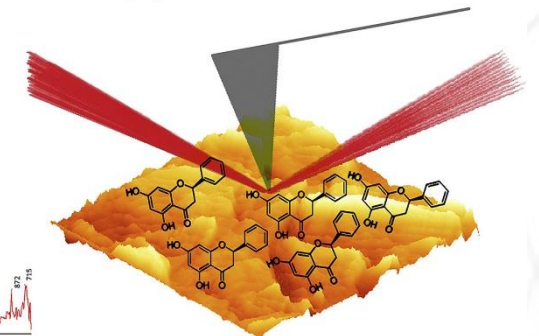
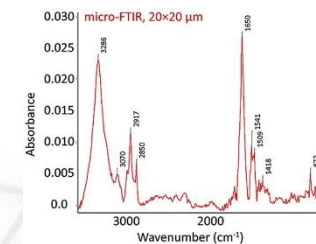
Reference autoFL, $\lambda_{exc} = 275 \text{ nm}$



- **Near-field measurements**
 - Detector-sample distance \ll wavelength
 - Diffraction does not occur in the near-field
- Nanometer resolution
- Sample constraints
 - Ultrathin samples
 - Ultrasmooth samples (rugosity $< 1 \mu\text{m}$)
- Nano IR couple AFM probes with IR beam
- Several measurement modes
 - Micro-thermocouples
 - Photothermal AFM-IR
 - Scattering Surface Near Field Optical Microscopy (sSNOM)
- IR sources
 - QCL
 - OPO
 - **Synchrotrons**



FTIR > FTIR microscopy > nano-FTIR
AFM-IR
SNOM



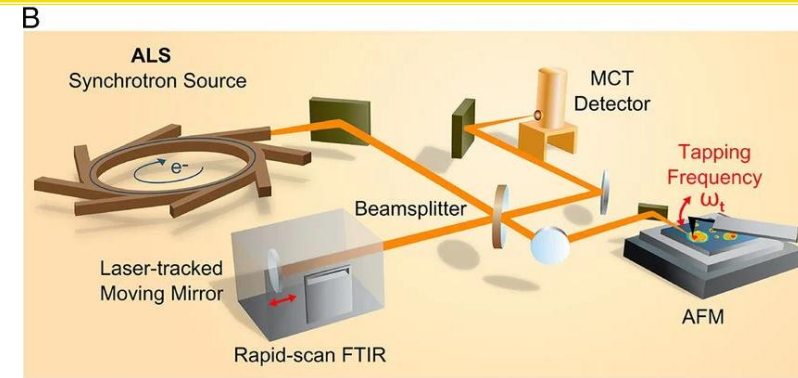
- Compatible with synchrotron source

- AFM IR

- Photothermal
- For soft materials

- scattering SNOM

- Scattering
- For hard materials



Bechtel et al.

Resonance Enhanced AFM-IR and Tapping AFM-IR

High speed, pulsed, tunable IR laser light is focused onto the sample at the AFM tip location. When IR wavelength matches the material absorbance bands, rapid thermal expansion occurs.

This expansion excites cantilever oscillations which are measured by the AFM. Laser repetition rate is matched to a resonance of the cantilever, achieving maximum sensitivity.

Spectra achieved by measuring cantilever oscillation amplitude as a function of IR wavelength creating a unique chemical fingerprint.

<10nm, high resolution, chemical images obtained by Tapping AFM-IR imaging at selected absorbing wavelengths.

AFM-IR also provides simultaneous topography, chemical and mechanical property mapping.

©2016 Anasys Instruments

Infrared scattering scanning nearfield optical microscopy

Incident IR light is focused under the AFM tip apex, and the scattered light carrying the optical properties of the sample is collected.

The localized light-matter interaction under the AFM tip can provide Sub-10nm spatial resolution.

With interferometric detection, both the amplitude and phase imaging of a sample at a given wavelength can be achieved.

By scanning across the sample while detecting the elastically scattered light, the optical response of the sample is imaged.

Bruker website

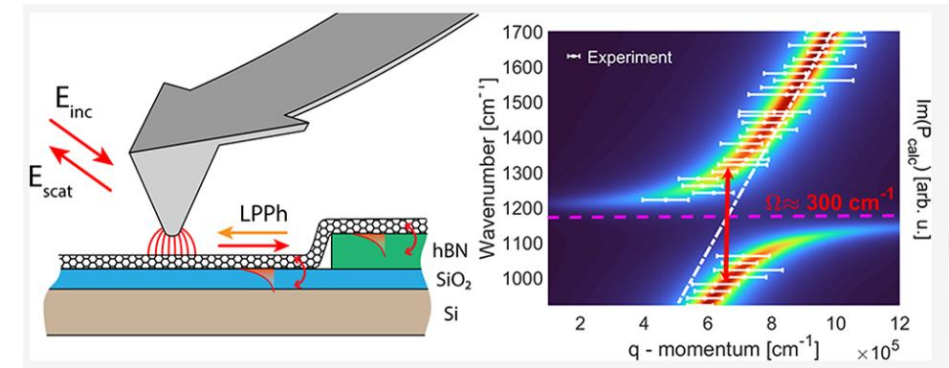
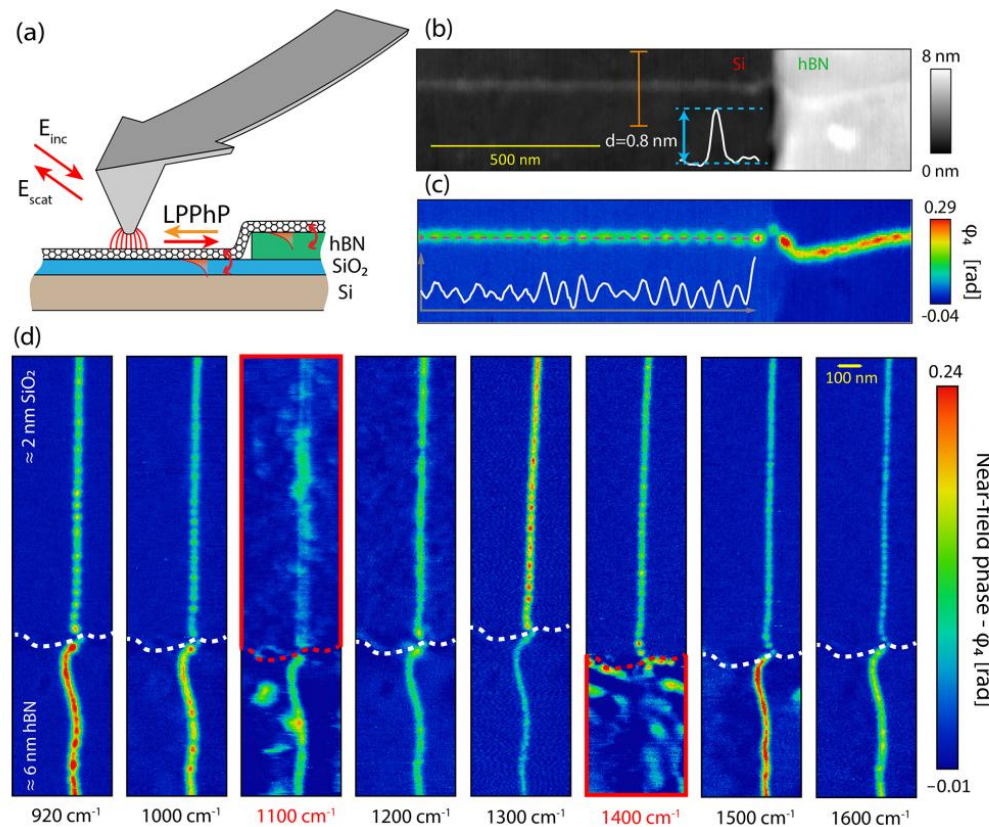
Sub-10nm resolution optical and chemical imaging

nanoFTIR spectroscopy

s-SNOM and Tapping AFM-IR



- One dimensional plasmon coupling in metallic carbon nanotubes



Direct Visualization of Ultrastrong Coupling between LuttingerLiquid Plasmons and Phonon Polaritons
 Gergely Németh,* Keigo Otsuka, Dániel Datz, Áron Pekker, Shigeo Maruyama, Ferenc Borondics,*
 and Katalin Kamarás, Nano Lett 2022

Thanks for your attention



The end

